SELF-ADAPTIVE hp-FEM

Waveguide example with six iris

Geometry of a cross section of the rectangular waveguide

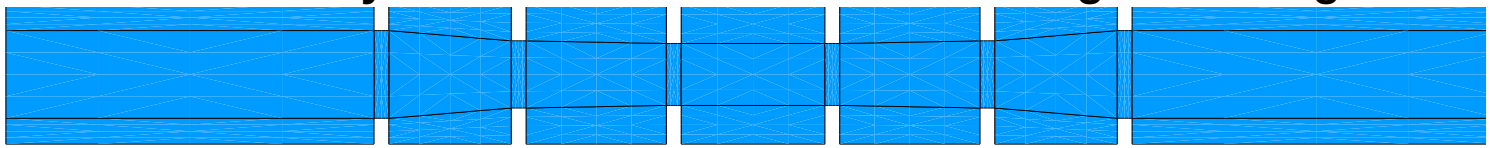

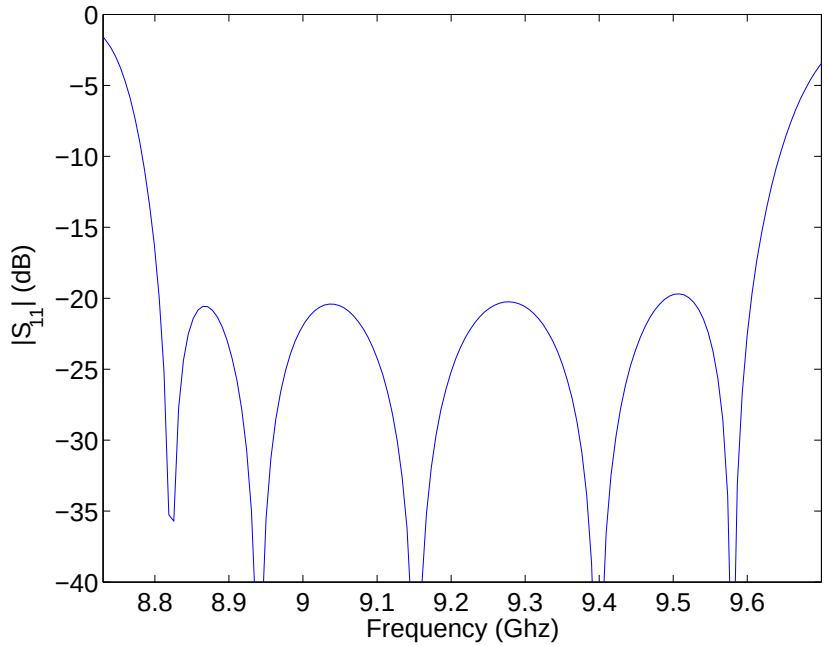

RETURN LOSS OF THE WAVEGUIDE

H-plane six resonant iris filter.

Dominant mode (source): $TE_{10}-$**mode.**

Dimensions $\approx 20 \times 2 \times 1$ **cm.**

Operating Frequency $\approx 8.8 - 9.6$ **Ghz**

Cutoff frequency ≈ 6.56 **Ghz**

SELF-ADAPTIVE hp-FEM

Griding Techniques for the Waveguide Problem

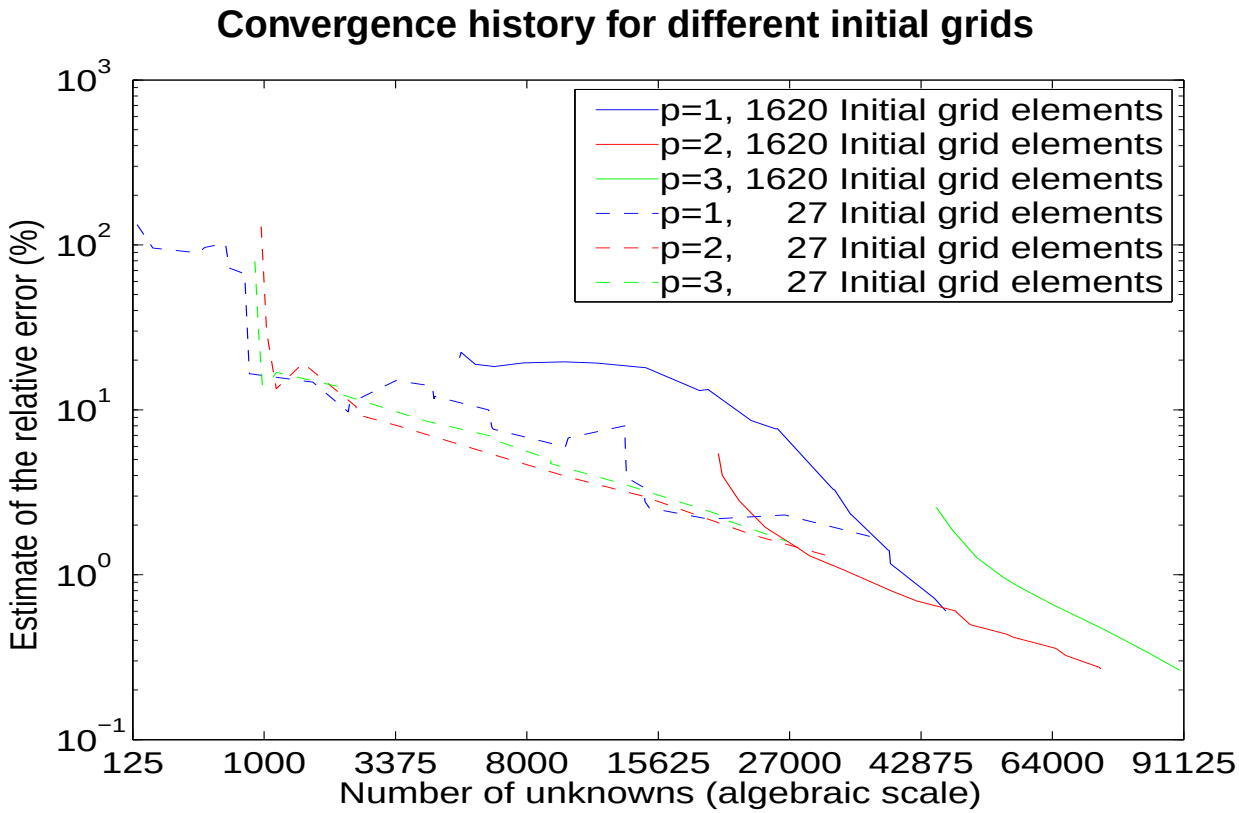

Conclusion : **Regardless of the initial grid, we obtain exponential convergence.**

SELF-ADAPTIVE hp-FEM

FEM solution for frequency $= 8.72$ Ghz

$|H_x|$

$|H_y|$

$\sqrt{|H_x|^2+|H_y|^2}$

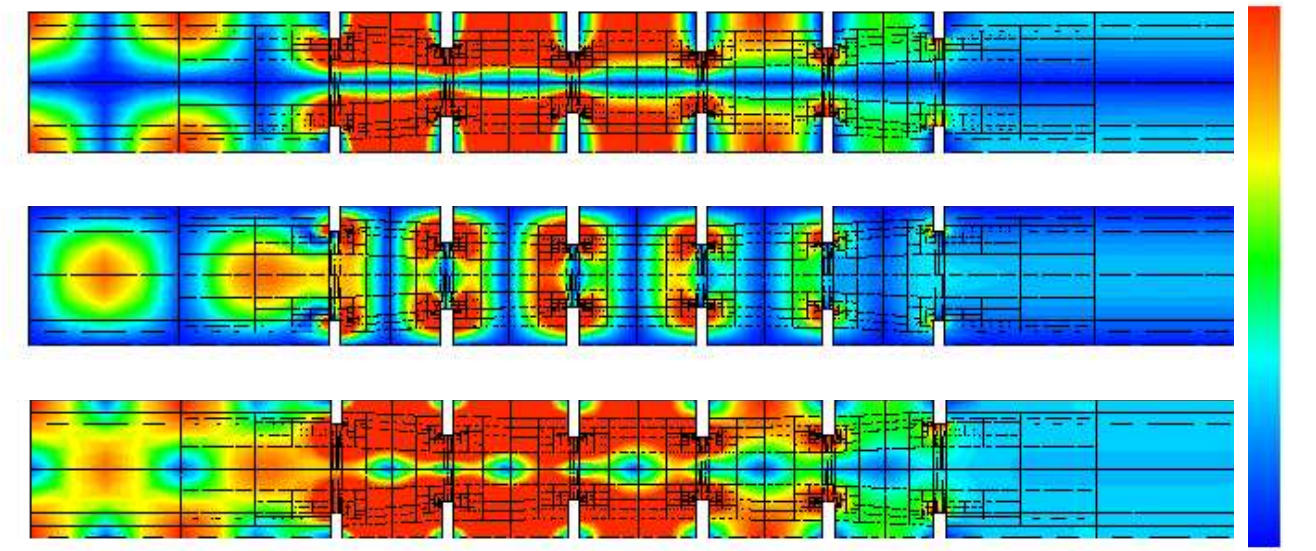

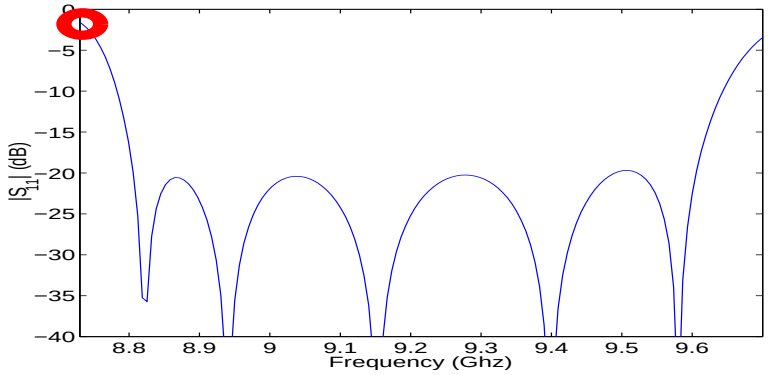

SELF-ADAPTIVE hp-FEM

FEM solution for frequency $= 8.82$ Ghz

$|H_x|$

$|H_y|$

$\sqrt{|H_x|^2+|H_y|^2}$

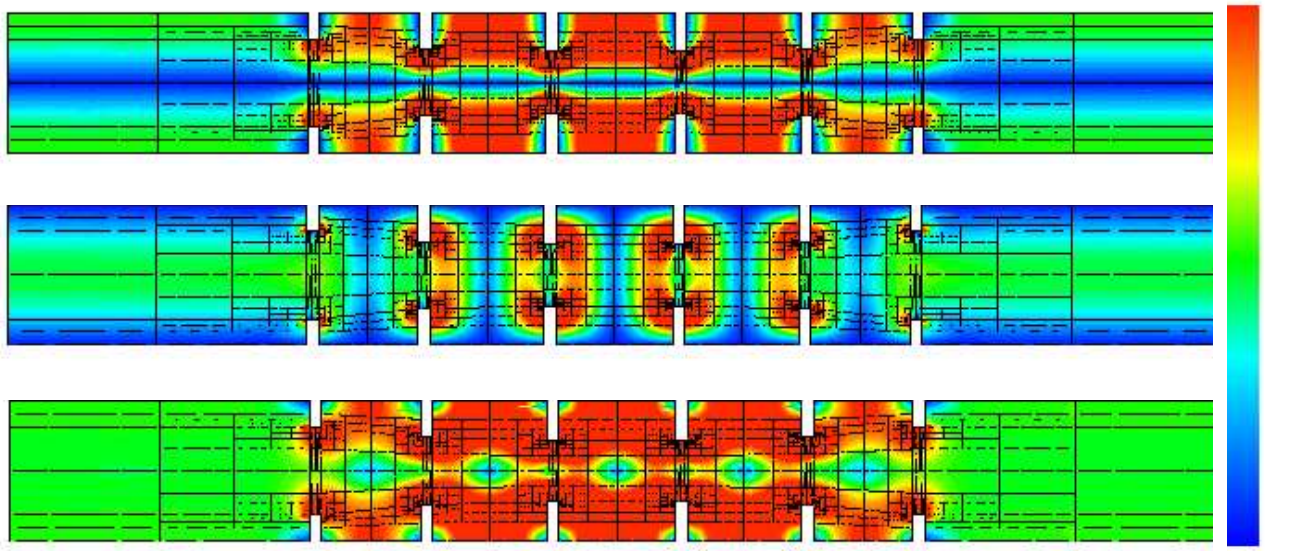

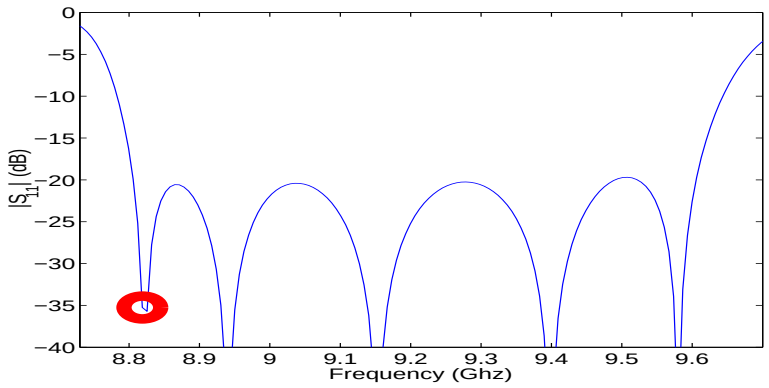

SELF-ADAPTIVE hp-FEM

FEM solution for frequency $= 9.58$ Ghz

$|H_x|$

$|H_y|$

$\sqrt{|H_x|^2+|H_y|^2}$

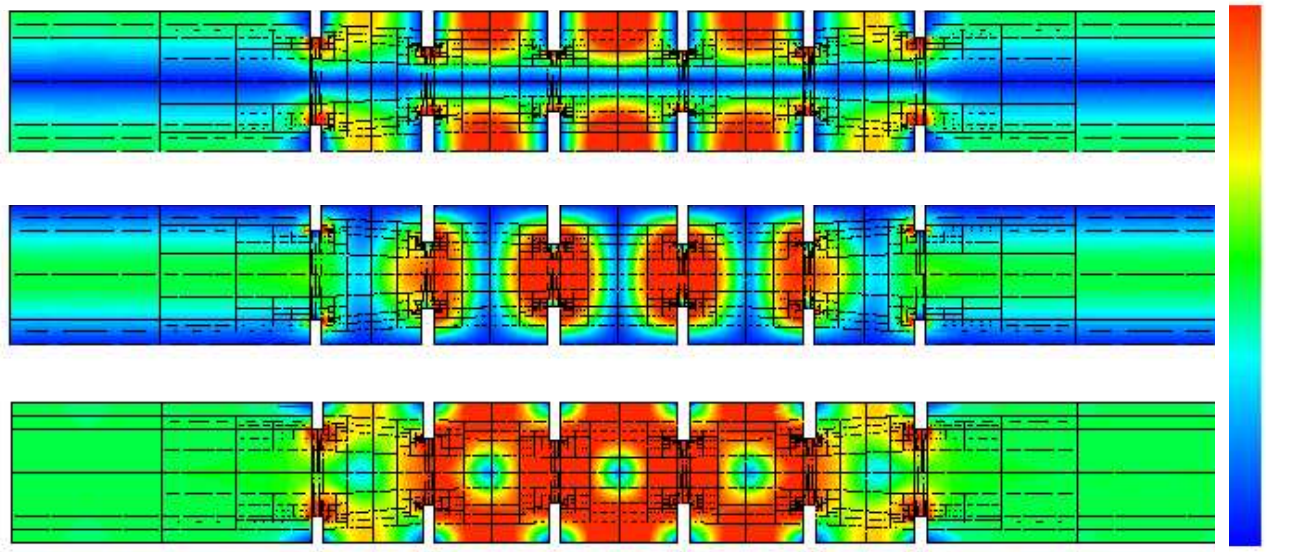

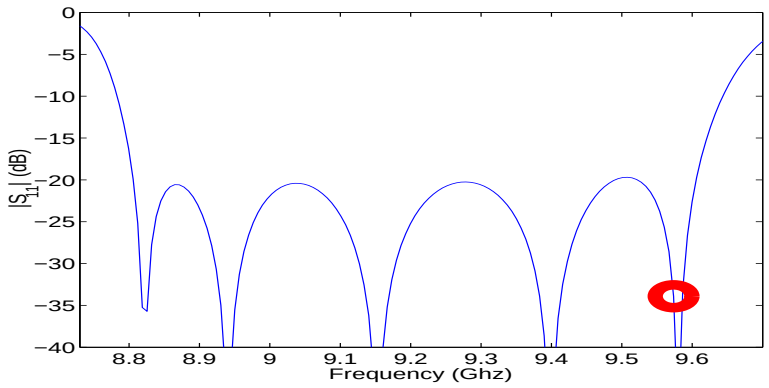

SELF-ADAPTIVE hp-FEM

FEM solution for frequency $= 9.71$ Ghz

$|H_x|$

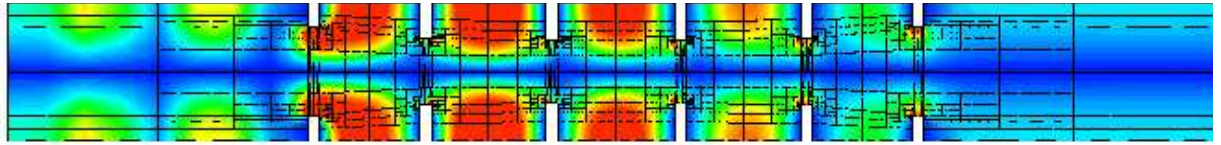

$|H_y|$

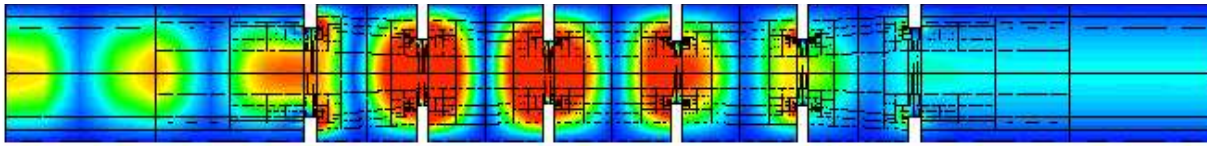

$\sqrt{|H_x|^2+|H_y|^2}$

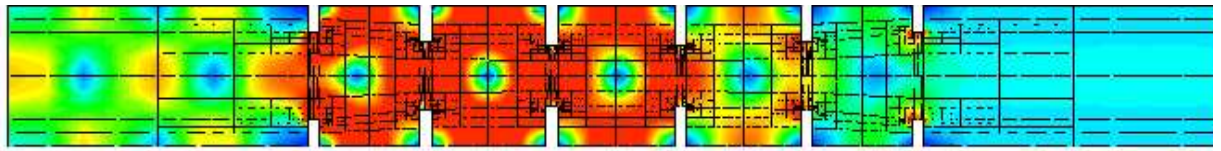

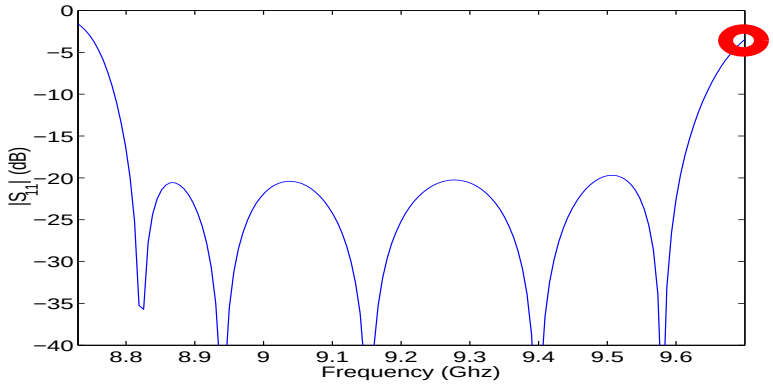

SELF-ADAPTIVE GOAL-ORIENTED hp-FEM

Motivation (Goal-Oriented Adaptivity)

Test Problem

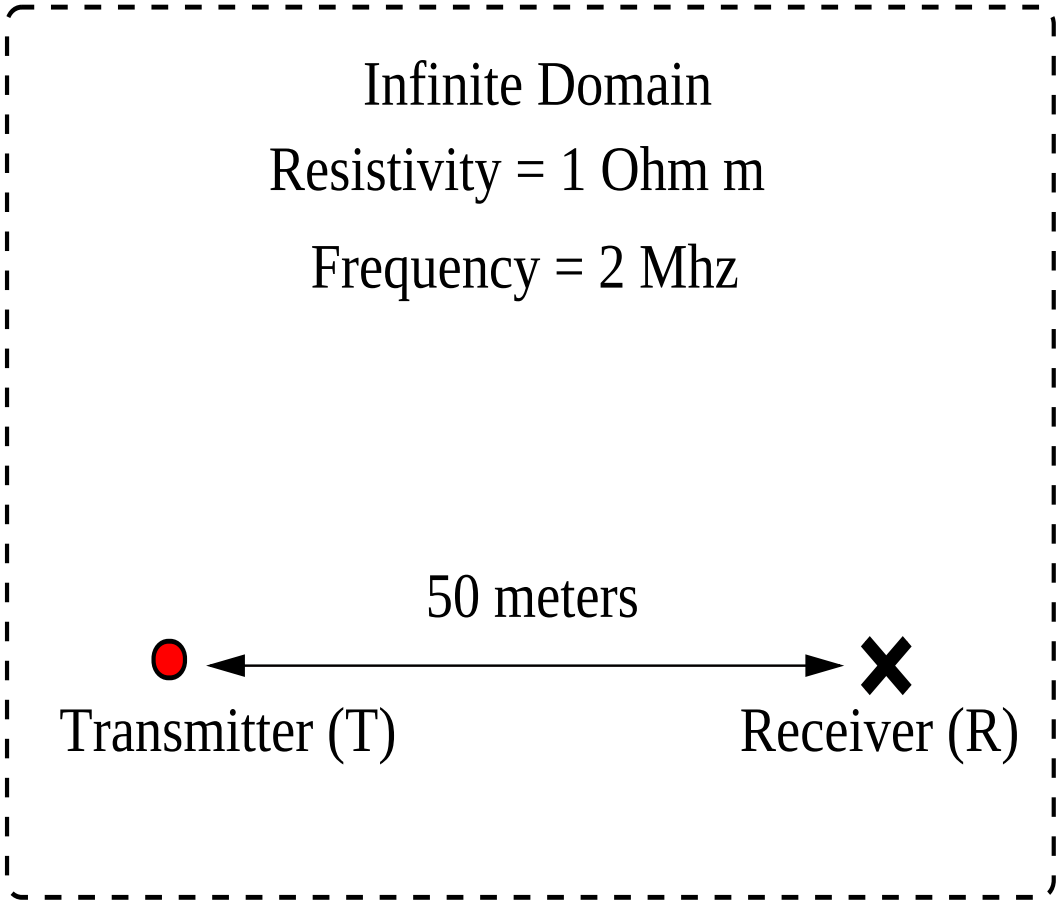

SELF-ADAPTIVE GOAL-ORIENTED hp-FEM

Motivation (Goal-Oriented Adaptivity)

Test Problem

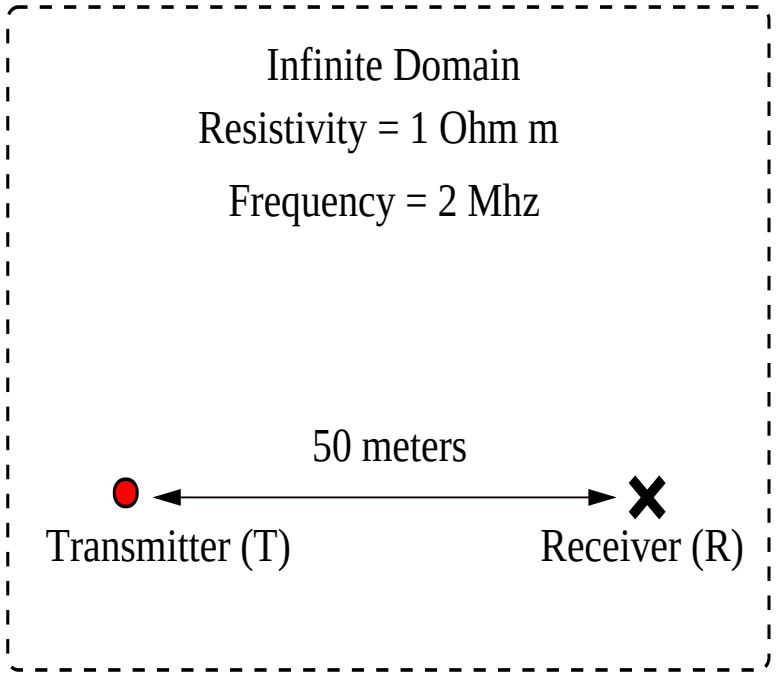

- **Solution decays exponentially.**
- $\dfrac{|\boldsymbol{E}(\boldsymbol{T})|}{|\boldsymbol{E}(\boldsymbol{R})|} \approx 10^{60}$
- **Results using energy-norm adaptivity:**
  - **Energy-norm error:** 0.001%
  - **Relative error in the quantity of interest** $> 10^{30}$ **%.**

SELF-ADAPTIVE GOAL-ORIENTED hp-FEM

Motivation (Goal-Oriented Adaptivity)

Test Problem

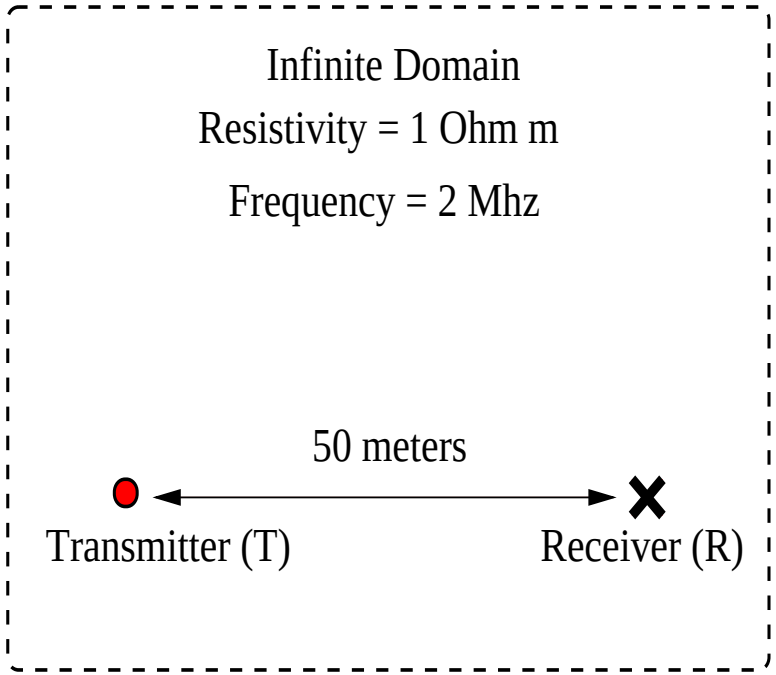

- **Solution decays exponentially.**
- $\dfrac{|\boldsymbol{E}(\boldsymbol{T})|}{|\boldsymbol{E}(\boldsymbol{R})|} \approx 10^{60}$
- **Results using energy-norm adaptivity:**
  - **Energy-norm error:** 0.001%
  - **Relative error in the quantity of interest** $> 10^{30}$ **%.**

Goal-oriented adaptivity is needed

Becker-Rannacher (1995,1996), Rannacher-Stuttmeier (1997), Cirak-Ramm (1998), Paraschivoiu-Patera (1998), Peraire-Patera (1998), Prudhomme-Oden (1999, 2001), Heuveline-Rannacher (2003), Solin-Demkowicz (2004).

SELF-ADAPTIVE GOAL-ORIENTED hp-FEM

Motivation (Goal-Oriented Adaptivity)

Test Problem

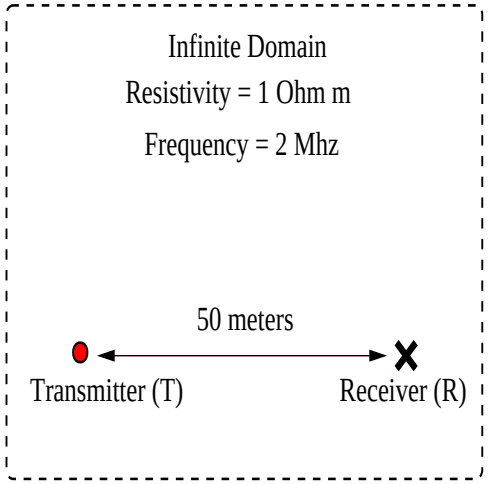

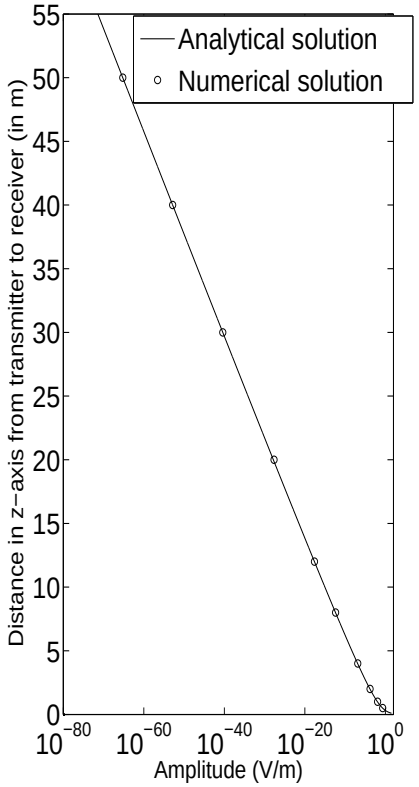

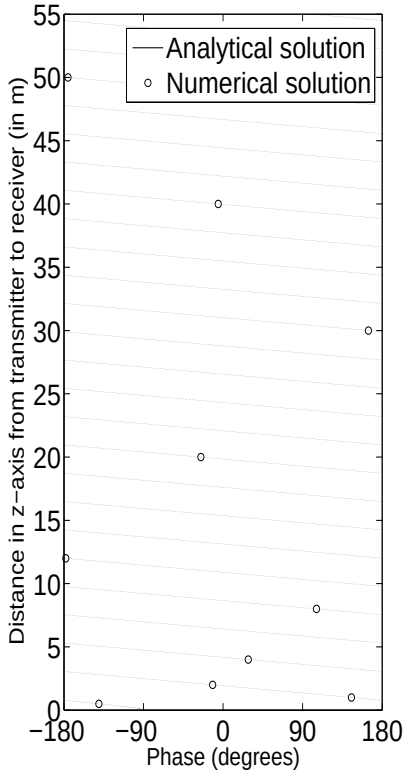

Goal-oriented adaptivity is needed

SELF-ADAPTIVE GOAL-ORIENTED hp-FEM

Motivation (Goal-Oriented Adaptivity)

Goal-Oriented adaptivity is a GENERALIZATION of Energy-norm adaptivity.

- **For a number of problems, goal-oriented adaptivity is exactly the same as energy-norm adaptivity.**
- **For other problems, the use of goal-oriented adaptivity becomes ESSENTIAL.**

To solve a problem with goal-oriented adaptivity is ALWAYS BETTER (or equal) than solving the problem with energy-norm adaptivity.

Short Course: Computing with hp-Elements

8th U.S. National Congress on Computational Mechanics.

Fully Automatic Goal-Oriented hp-Adaptive Strategy for Simulating Resistivity Logging Instruments

David Pardo (dzubiaur@yahoo.es),
L. Demkowicz, C. Torres-Verdin

Collaborators: Science Department of Baker-Atlas, L. Tabarovsky
J. Kurtz, M. Paszynski, D. Xue, W. Rachowicz

July 28, 2005

Department of Petroleum and Geosystems Engineering, and
Institute for Computational Engineering and Sciences (ICES)
The University of Texas at Austin

OVERVIEW

1. **Motivation for Using Goal-Oriented Adaptivity.**
2. **Introduction to Resistivity Logging Instruments.**
3. **The Self-Adaptive Goal-Oriented hp-Algorithm.**
   - **Main Idea.**
   - **Mathematical Formulation.**
   - **Algorithm and Implementation.**
4. **Numerical Results:**
   - **Simulation of Resistivity Logging Instruments with Mandrel.**
   - **Simulation of Resistivity Logging Instruments with Casing.**
5. **Conclusions and Future Work (3D Problems, Multi-physics).**

RESISTIVITY LOGGING INSTRUMENTS

Logging Instruments: Definition

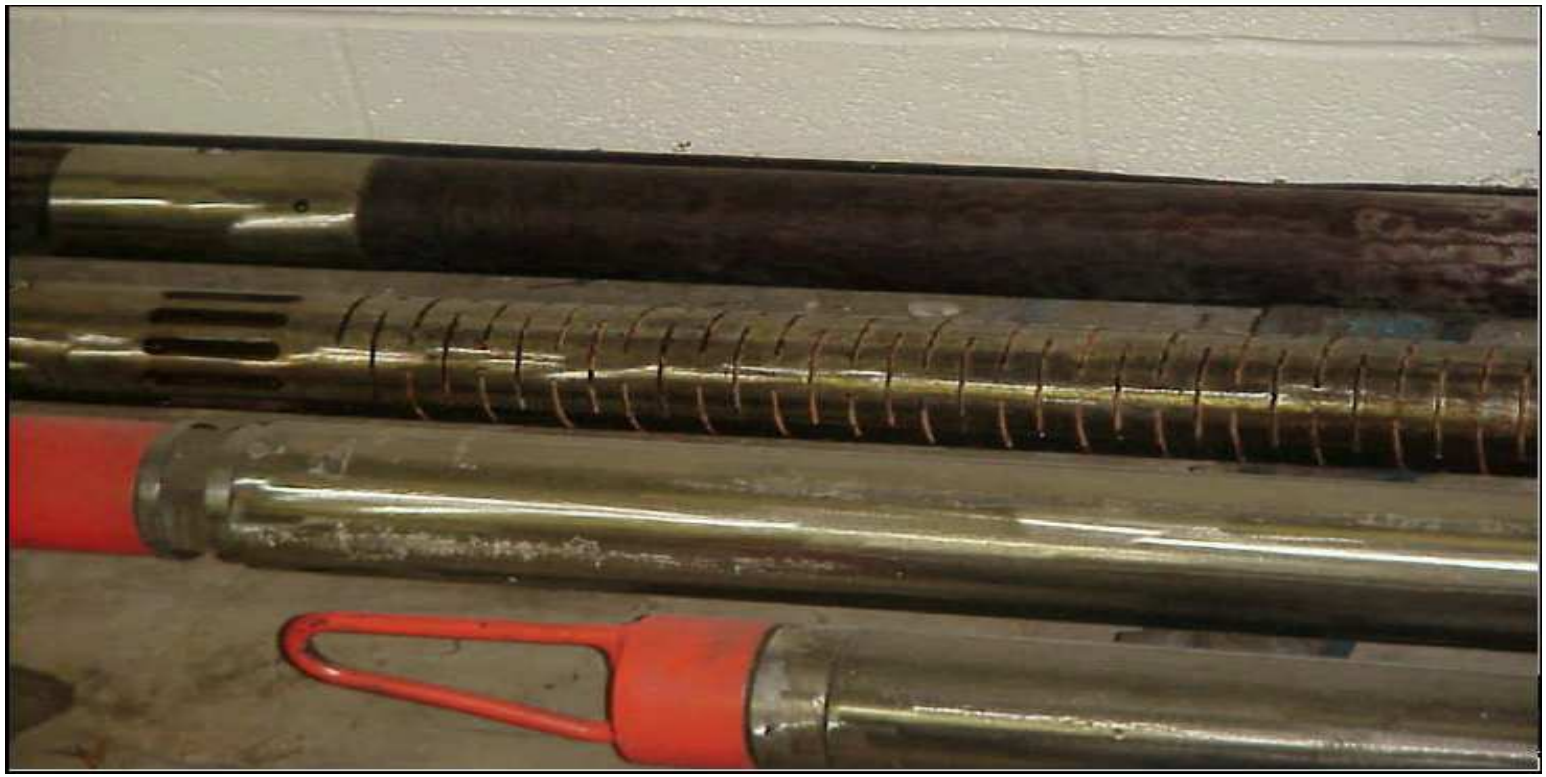

RESISTIVITY LOGGING INSTRUMENTS

Utility of Logging Instruments

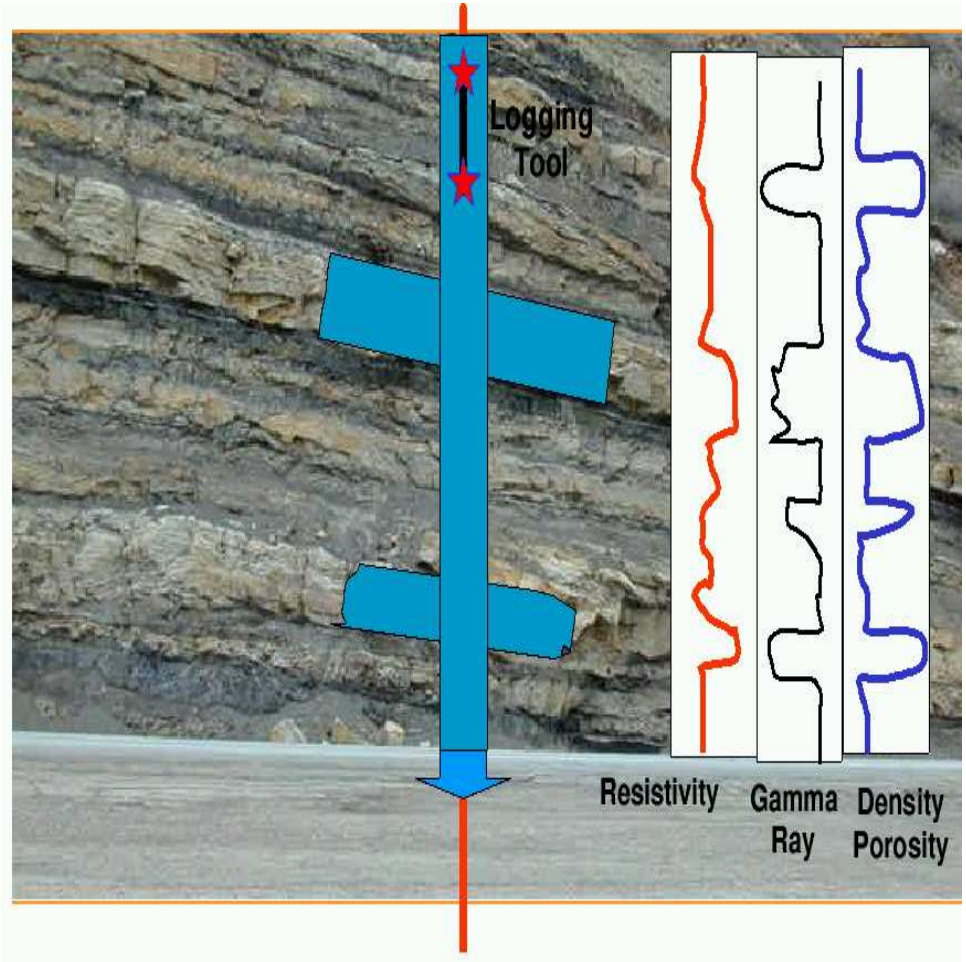

OBJECTIVES: To determine

- **Payzones (oil and gas).**
- **Amount of oil/gas.**
- **Ability to extract oil/gas.**

$

RESISTIVITY LOGGING INSTRUMENTS

Main Objective: To Solve an Inverse Problem

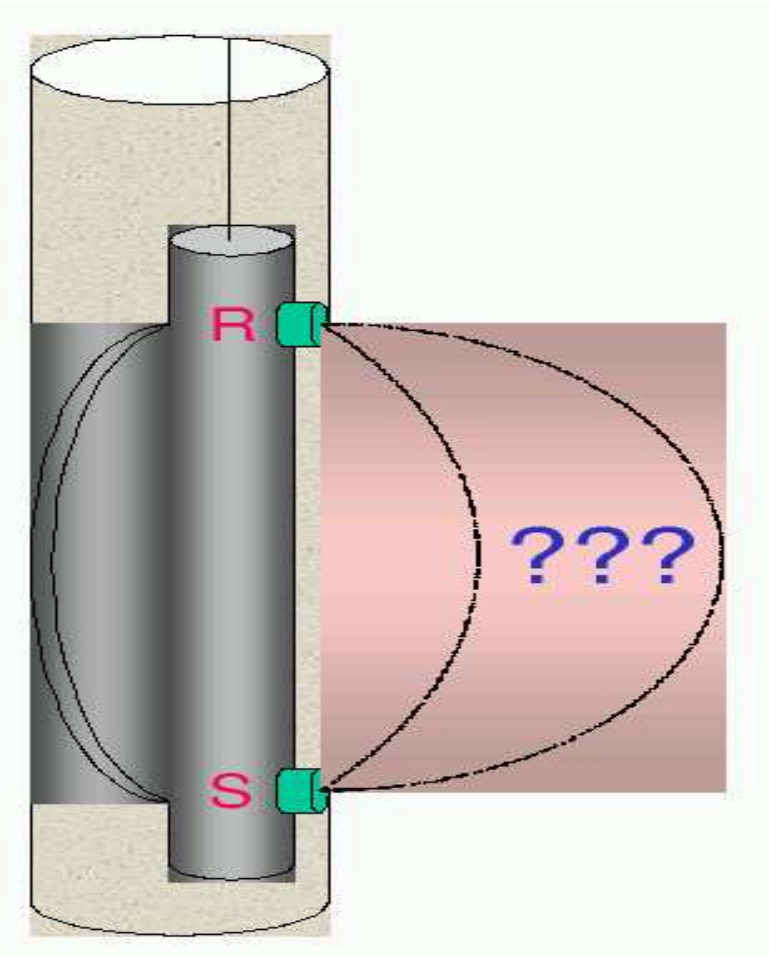

A software for solving the DIRECT problem is essential in order to solve the INVERSE problem

RESISTIVITY LOGGING INSTRUMENTS

Resistivity Logging Instruments

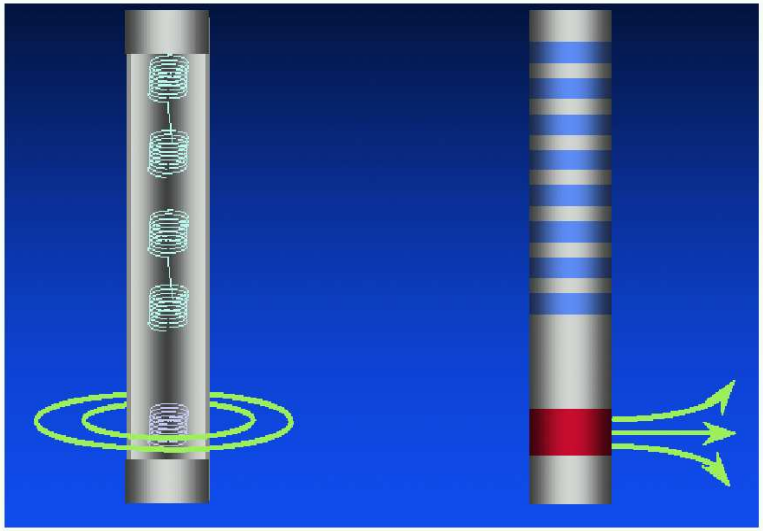

RESISTIVITY LOGGING INSTRUMENTS

Final Result Obtained from the Logging Instruments

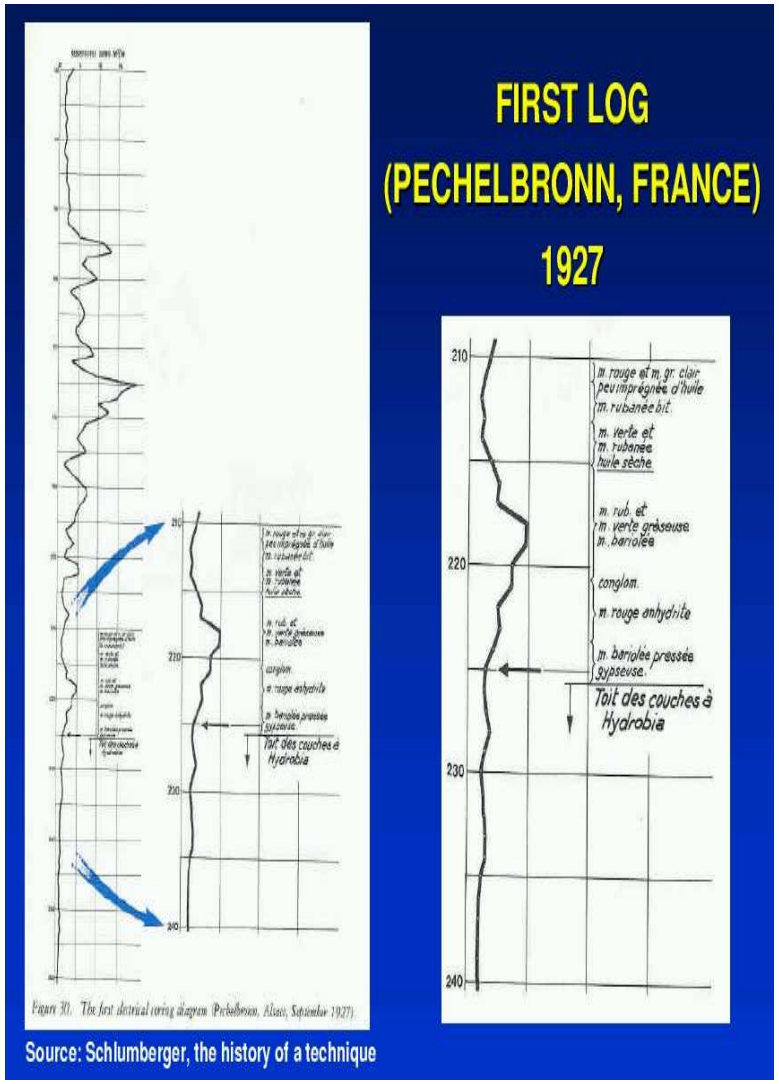

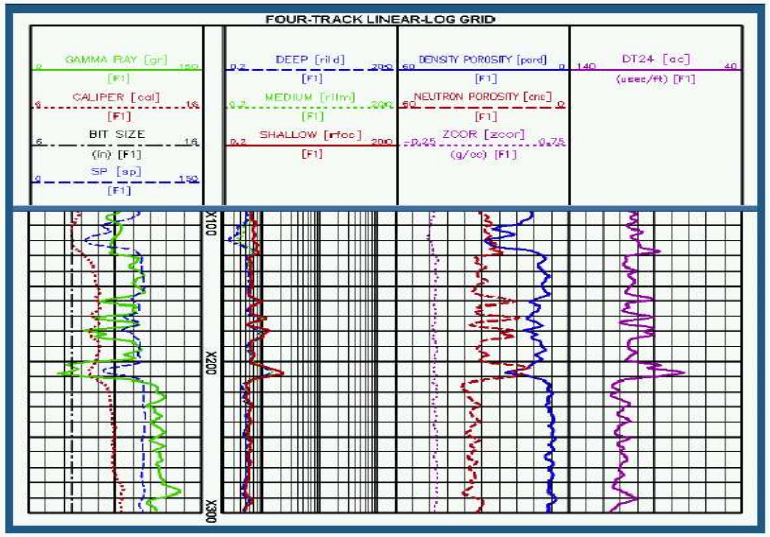

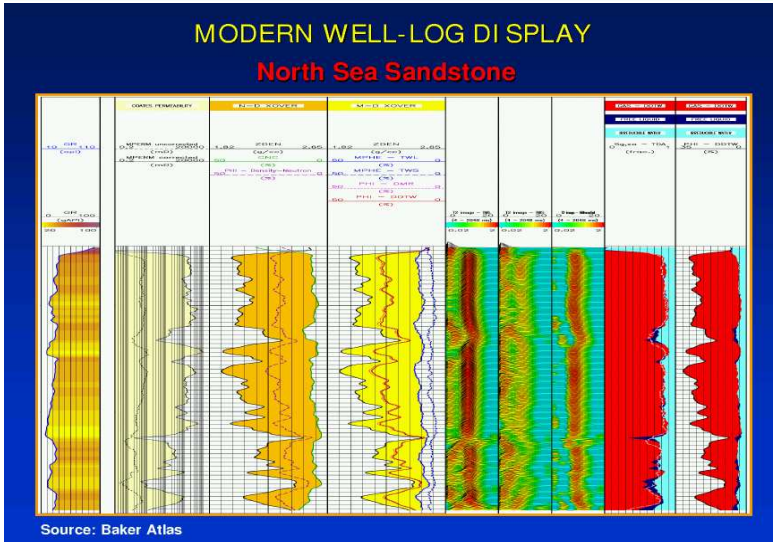

RESISTIVITY LOGGING INSTRUMENTS

Electromagnetism

Time-Harmonic Maxwell's Equations

$\nabla \times \mathrm{H} = (\bar{\bar{\sigma}} + j\omega\bar{\bar{\epsilon}})\mathrm{E} + \mathrm{J}^{imp}$	**Ampere's law**
$\nabla \times \mathrm{E} = -j\omega\bar{\bar{\mu}}\mathrm{H} - \mathrm{M}^{imp}$	**Faraday's law**
$\nabla \cdot (\bar{\bar{\epsilon}}\mathrm{E}) = \rho$	**Gauss' law of Electricity**
$\nabla \cdot (\bar{\bar{\mu}}\mathrm{H}) = 0$	**Gauss' law of Magnetism**

E-VARIATIONAL FORMULATION:

$$\left\{ \begin{array}{l} \text{Find } \mathrm{E} \in \mathrm{E}_D + \boldsymbol{H}_D(\mathrm{curl};\Omega) \text{ such that:} \\ \displaystyle\int_\Omega (\bar{\bar{\mu}}^{-1}\nabla \times \mathrm{E}) \cdot (\nabla \times \bar{\mathrm{F}})\, dV - \int_\Omega (\bar{\bar{k}}^2 \mathrm{E}) \cdot \bar{\mathrm{F}}\, dV = -j\omega \int_\Omega \mathrm{J}^{imp} \cdot \bar{\mathrm{F}}\, dV \\ \displaystyle +j\omega \int_{\Gamma_N} \mathrm{J}^{imp}_{\Gamma_N} \cdot \bar{\mathrm{F}}_t\, dS - \int_\Omega (\bar{\bar{\mu}}^{-1}\mathrm{M}^{imp}) \cdot (\nabla \times \bar{\mathrm{F}})\, dV \quad \forall\, \mathrm{F} \in \boldsymbol{H}_D(\mathrm{curl};\Omega) \end{array} \right.$$

RESISTIVITY LOGGING INSTRUMENTS

Variational Formulation

AXISYMMETRIC PROBLEMS

E_ϕ -Variational Formulation (Azimuthal)

Find $E_\phi \in E_{\phi,D} + \tilde{H}^1_D(\Omega)$ **such that:**

$$\int_\Omega (\bar{\bar{\mu}}^{-1}_{\rho,z} \nabla \times \mathrm{E}_\phi) \cdot (\nabla \times \bar{\mathrm{F}}_\phi)\, dV - \int_\Omega (\bar{\bar{k}}^2_\phi \mathrm{E}_\phi) \cdot \bar{\mathrm{F}}_\phi\, dV = -j\omega \int_\Omega J^{imp}_\phi\, \bar{F}_\phi\, dV$$
$$+j\omega \int_{\Gamma_N} J^{imp}_{\phi,\Gamma_N}\, \bar{F}_\phi\, dS - \int_\Omega (\bar{\bar{\mu}}^{-1}_{\rho,z} \mathrm{M}^{imp}_{\rho,z}) \cdot \bar{\mathrm{F}}_\phi\, dV \qquad \forall\, F_\phi \in \tilde{H}^1_D(\Omega)$$

$\mathrm{E}_{\rho,z}$ -Variational Formulation (Meridian)

Find $(E_\rho, E_z) \in \mathrm{E}_D + \tilde{H}_D(\mathrm{curl};\Omega)$ **such that:**

$$\int_\Omega (\bar{\bar{\mu}}^{-1}_{\phi} \nabla \times \mathrm{E}_{\rho,z}) \cdot (\nabla \times \bar{\mathrm{F}}_{\rho,z})\, dV - \int_\Omega (\bar{\bar{k}}^2_{\rho,z} \mathrm{E}_{\rho,z}) \cdot \bar{\mathrm{F}}_{\rho,z}\, dV =$$
$$-j\omega \int_\Omega J^{imp}_\rho \bar{F}_\rho + J^{imp}_z \bar{F}_z\, dV + j\omega \int_{\Gamma_N} J^{imp}_{\rho,\Gamma_N} \bar{F}_\rho + J^{imp}_{z,\Gamma_N} \bar{F}_z\, dS$$
$$- \int_\Omega (\bar{\bar{\mu}}^{-1}_{\phi} \mathrm{M}^{imp}_\phi) \cdot \bar{\mathrm{F}}_{\rho,z}\, dV \qquad \forall\, (F_\rho, F_z) \in \tilde{H}_D(\mathrm{curl};\Omega)$$

SELF-ADAPTIVE hp-FEM

Energy norm based fully automatic *hp*-adaptive strategy

Coarse grids
(hp)

Fine grids
($h/2, p+1$)

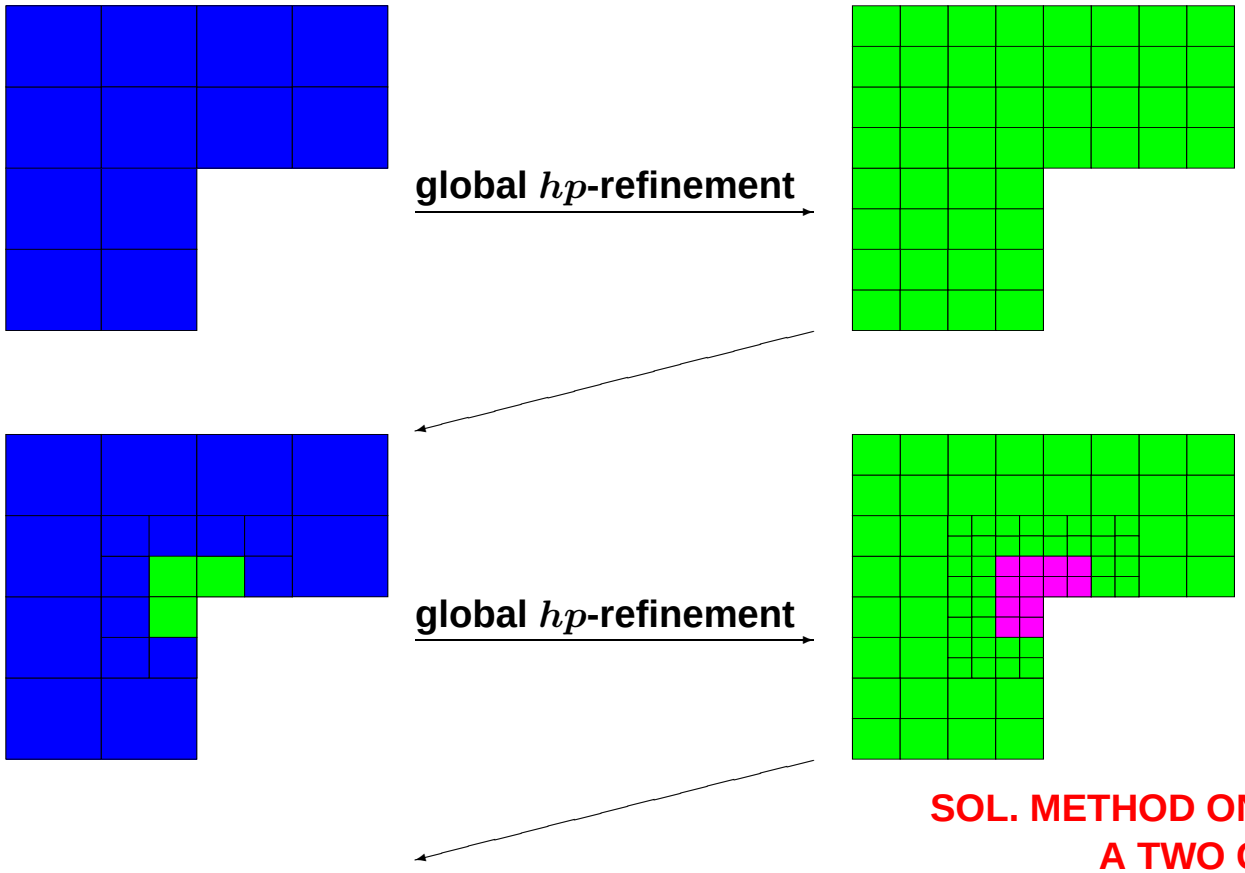

SOL. METHOD ON FINE GRIDS:
A TWO GRID SOLVER

SELF-ADAPTIVE GOAL-ORIENTED hp-FEM

Mathematical Formulation (Goal-Oriented Adaptivity)

We consider the following problem (in variational form):

$$\begin{cases} \text{Find } L(\Psi), \text{ where } \Psi \in V \text{ such that :} \\ b(\Psi, \xi) = f(\xi) \quad \forall \xi \in V \ . \end{cases}$$

We define residual $r_e(\xi) = b(e, \xi)$. We seek for solution G of:

$$\begin{cases} \text{Find } G \in V'' \sim V \text{ such that :} \\ G(r_e) = L(e) \ . \end{cases}$$

This is necessarily solved if we find the solution of the *dual* problem:

$$\begin{cases} \text{Find } G \in V \text{ such that :} \\ b(\Psi, G) = L(\Psi) \quad \forall \Psi \in V \ . \end{cases}$$

Notice that $L(e) = b(e, G)$.

SELF-ADAPTIVE GOAL-ORIENTED hp-FEM

Mathematical Formulation (Goal-Oriented Adaptivity)

DIRECT PROBLEM

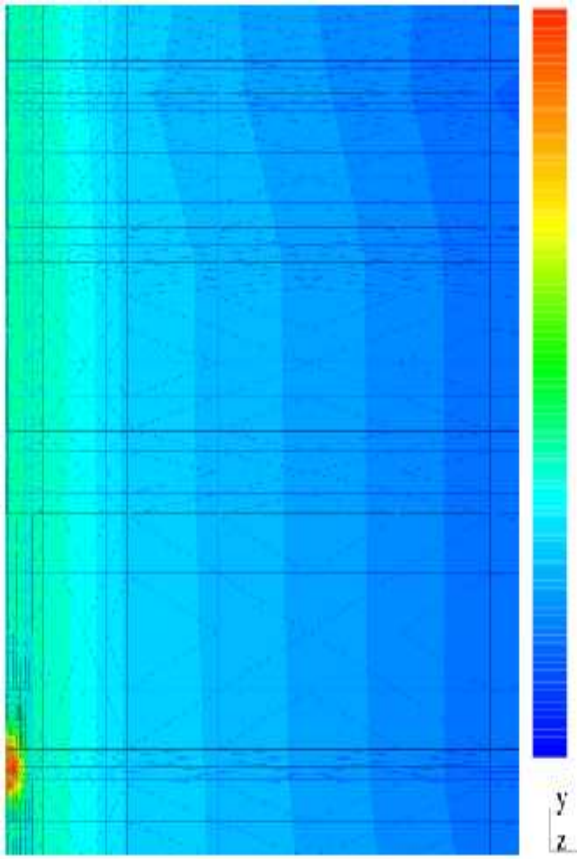

DUAL PROBLEM

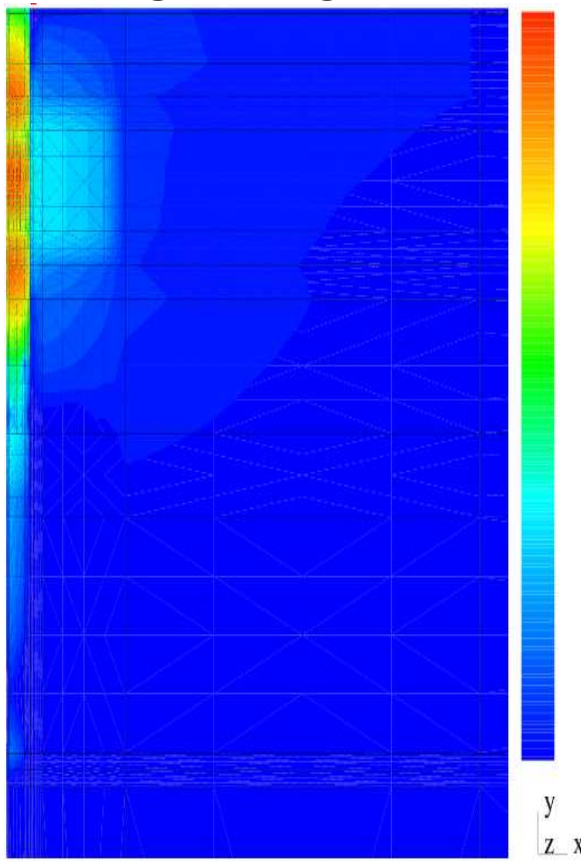

$$L(\Psi)=b(\Psi,G)$$

SELF-ADAPTIVE GOAL-ORIENTED hp-FEM

Algorithm for Goal-Oriented Adaptivity

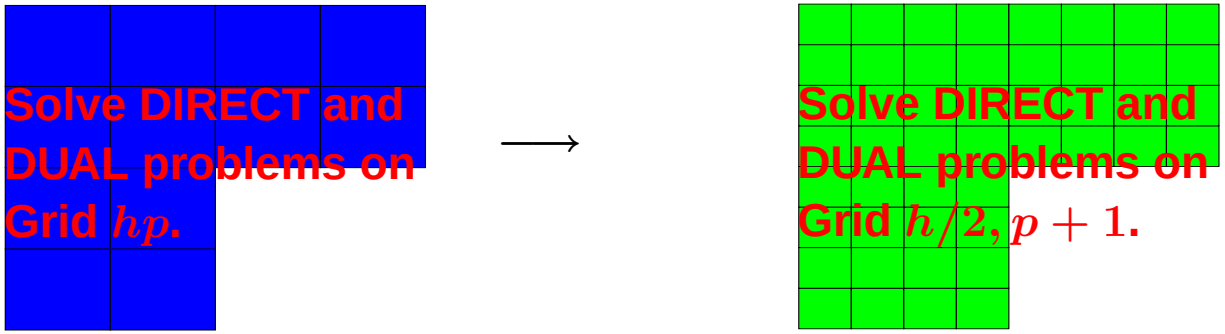

Compute $e = \Psi_{h/2,p+1} - \Psi_{hp}$, **and** $\tilde{e} = \Psi_{h/2,p+1} - \Pi_{hp}\Psi_{h/2,p+1}$.

Compute $\epsilon = G_{h/2,p+1} - G_{hp}$, **and** $\tilde{\epsilon} = G_{h/2,p+1} - \Pi_{hp}G_{h/2,p+1}$.

$$|L(e)| = |b(e,\epsilon)| \sim |b(\tilde{e},\tilde{\epsilon})| \leq \sum_K |b_K(\tilde{e},\tilde{\epsilon})| \leq \sum_K \| \tilde{e} \|_{E,K} \| \tilde{\epsilon} \|_{E,K}.$$

Apply the fully automatic hp-adaptive algorithm.

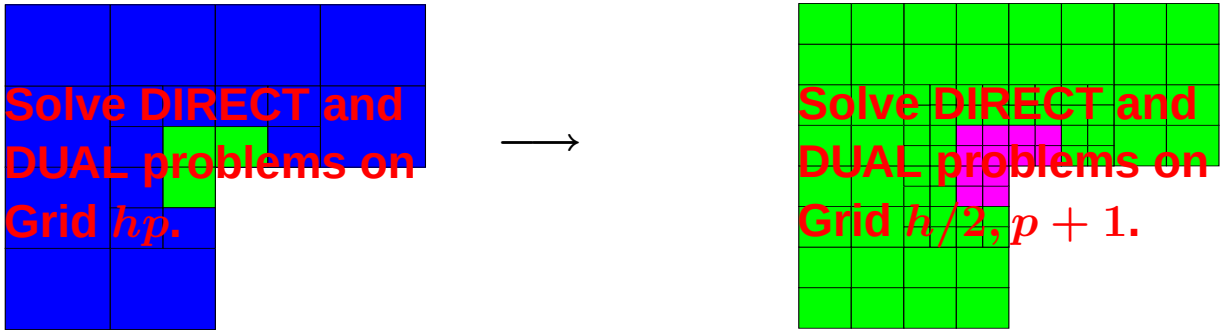

NUMERICAL RESULTS

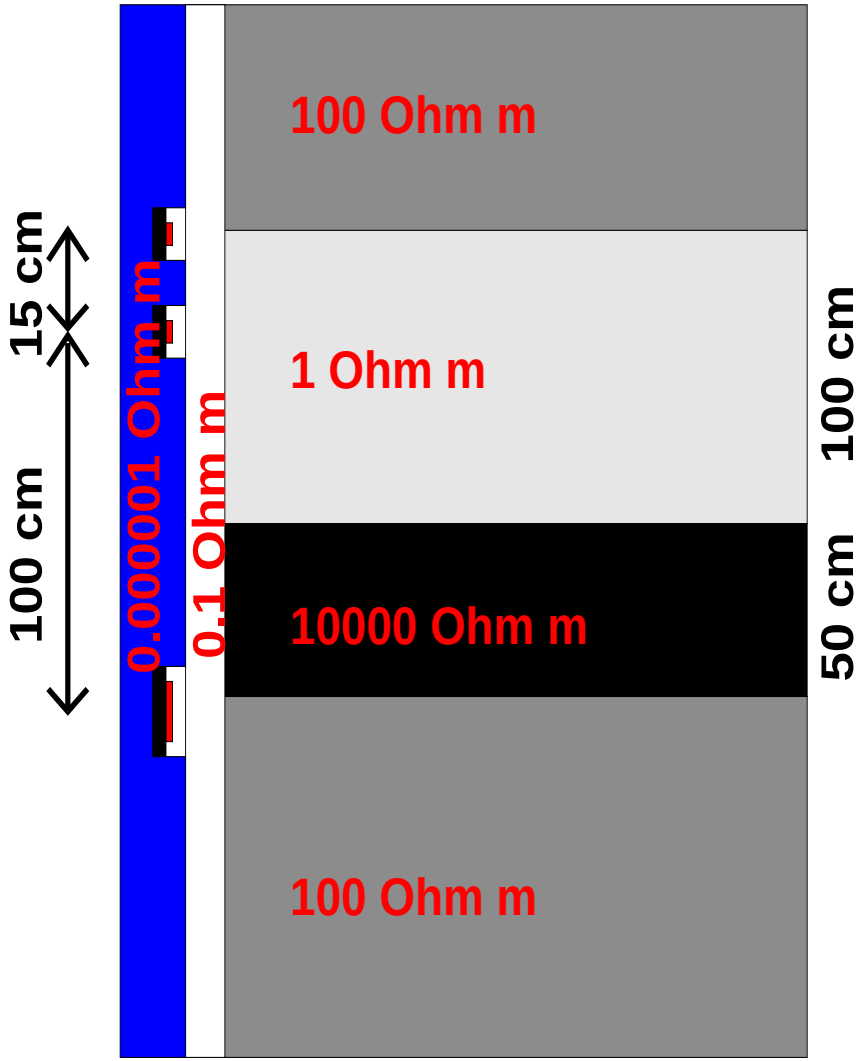

Description of Antennas

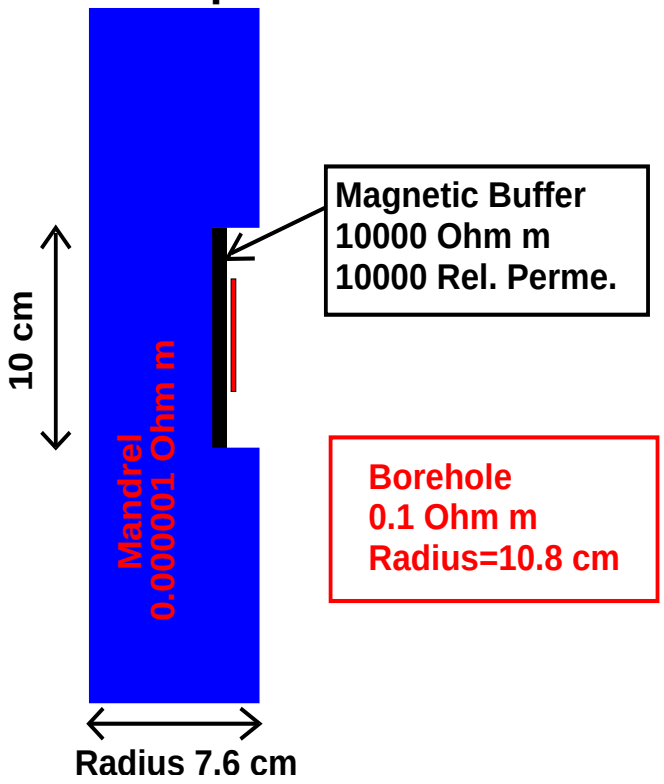

Goal: To Compute First Difference of Potential on Receiving Antennas

NUMERICAL RESULTS

First. Vert. Diff. E_ϕ (solenoid). Position: 0.475m

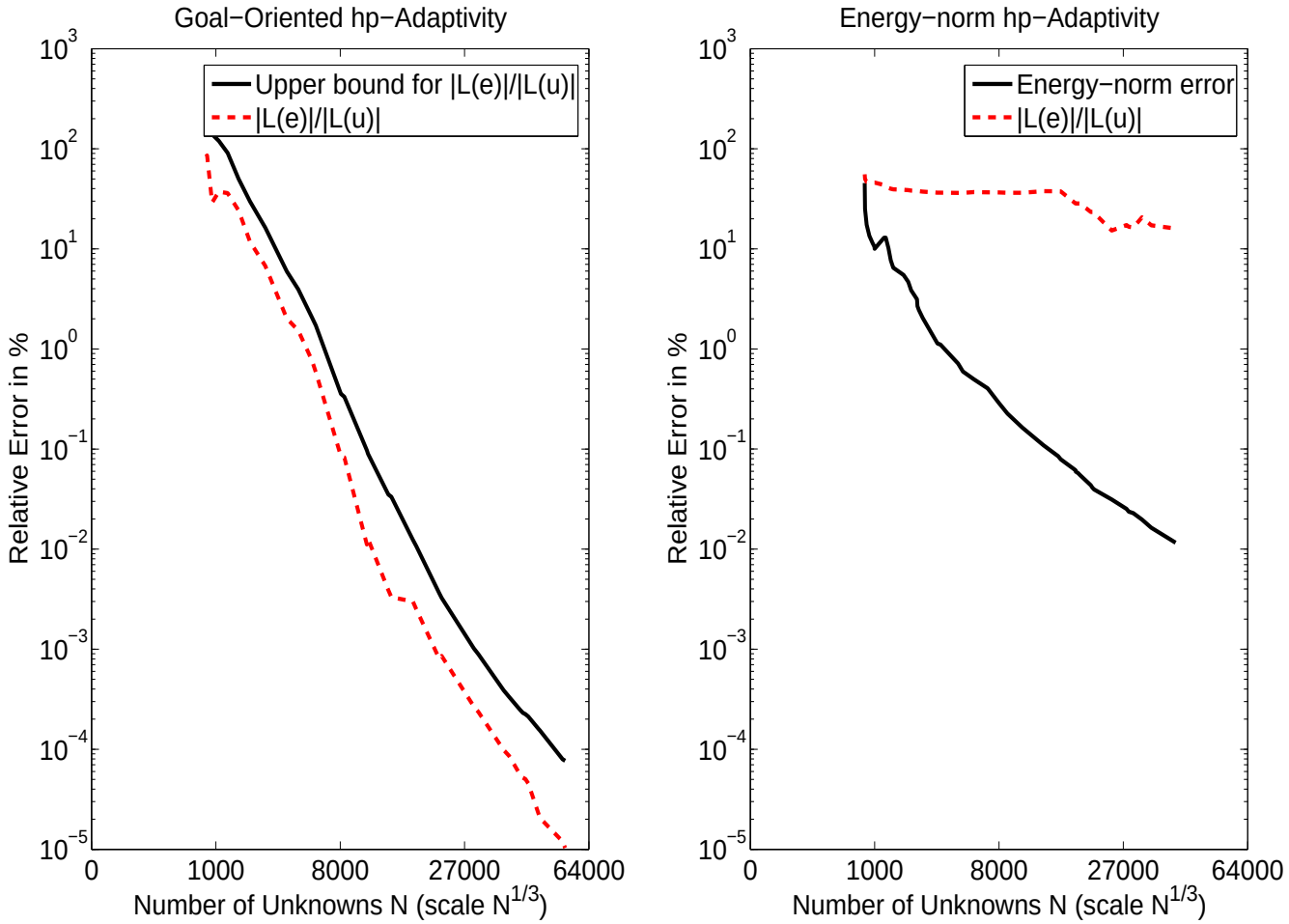

NUMERICAL RESULTS

Goal-Oriented vs. Energy-norm hp-Adaptivity

Problem with Mandrel at 2 Mhz.

Continuous Elements (Goal-Oriented Adaptivity)

Quantity of Interest	Real Part	Imag Part
COARSE GRID	-0.1629862203E-01	-0.4016944732E-02
FINE GRID	-0.1629862347E-01	-0.4016944223E-02

Continuous Elements (Energy-norm Adaptivity)

Quantity of Interest	Real Part	Imag Part
0.01% ENERGY ERROR	-0.1382759158E-01	-0.2989492851E-02

It is critical to use GOAL-ORIENTED adaptivity.

NUMERICAL RESULTS

First. Vert. Diff. E_ϕ (solenoid). Position: 0.475m

ENERGY-NORM HP-ADAPTIVITY

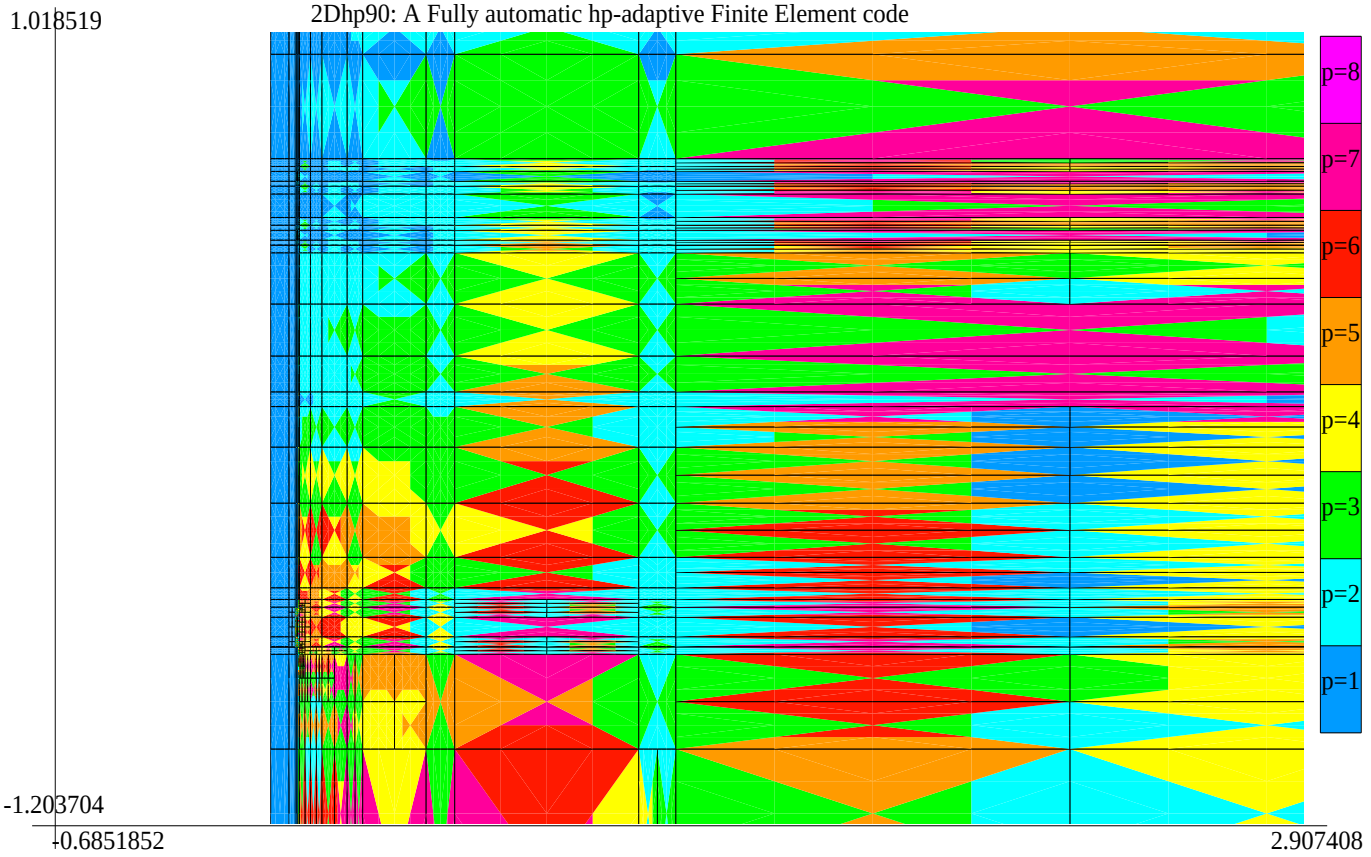

NUMERICAL RESULTS

First. Vert. Diff. E_ϕ (solenoid). Position: 0.475m

GOAL-ORIENTED HP-ADAPTIVITY

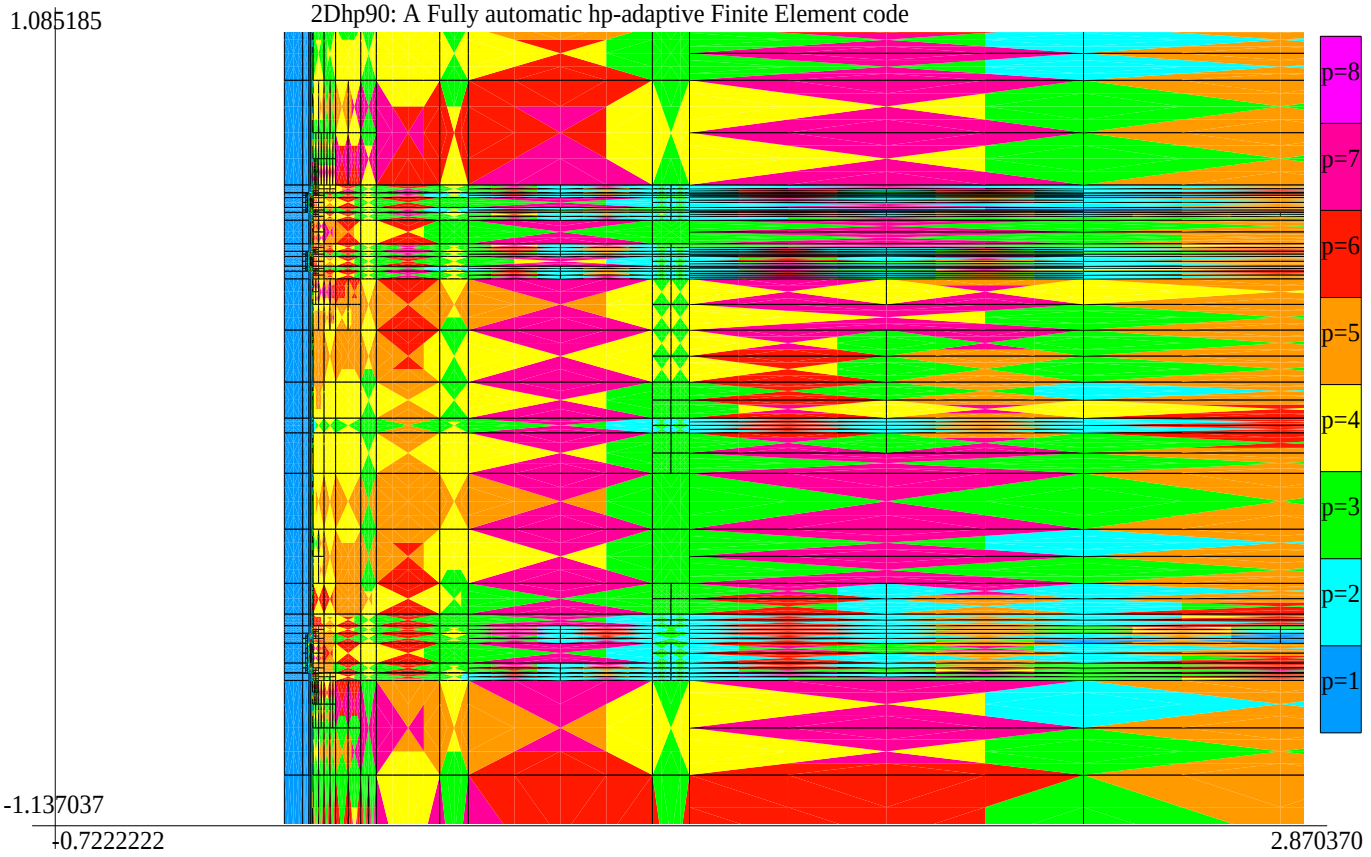

NUMERICAL RESULTS

First. Vert. Diff. E_ϕ (solenoid). Position: 0.475m

GOAL-ORIENTED HP-ADAPTIVITY (ZOOM TOWARDS FIRST RECEIVER ANTENNA)

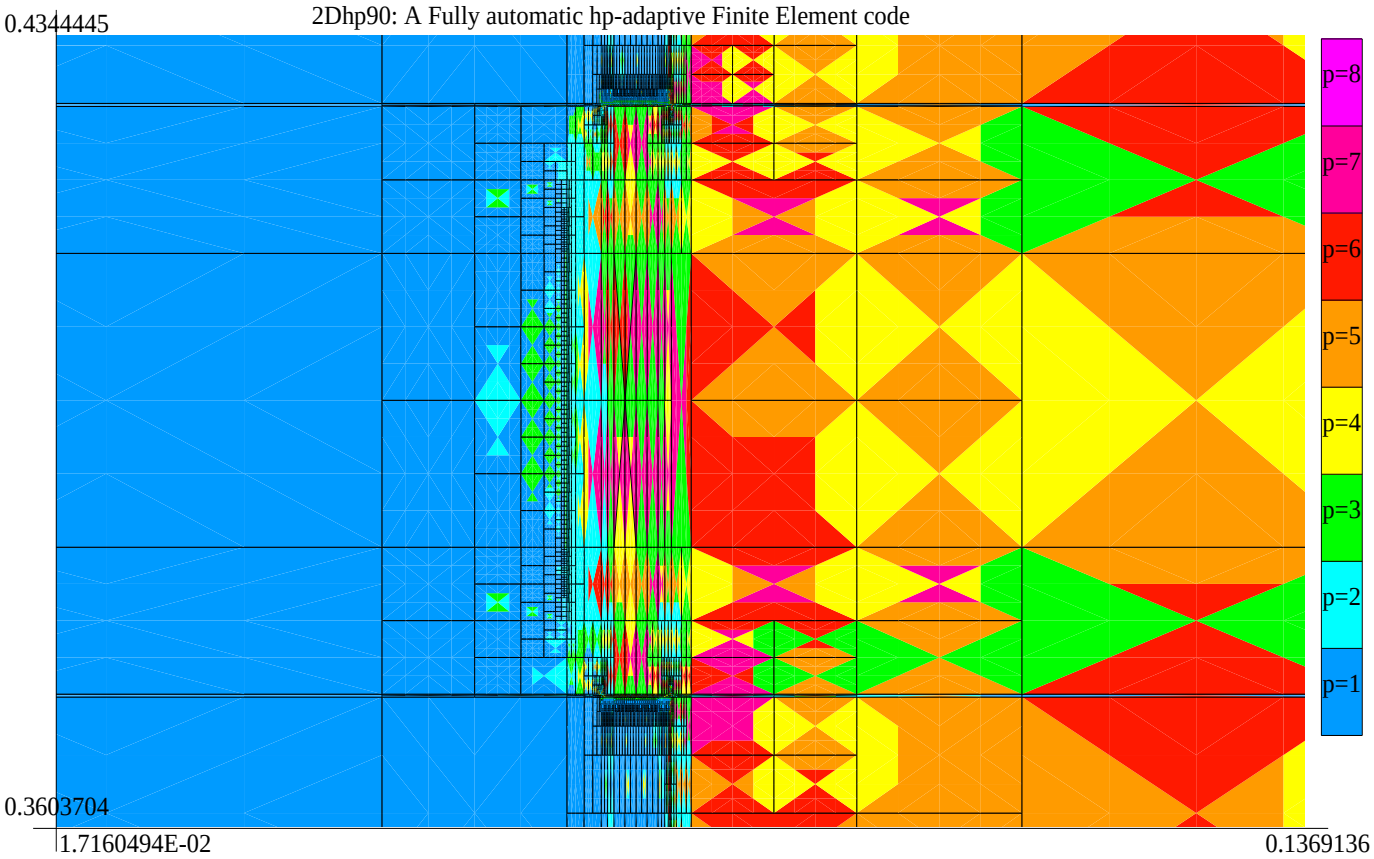

NUMERICAL RESULTS

E_ϕ for a solenoid antenna

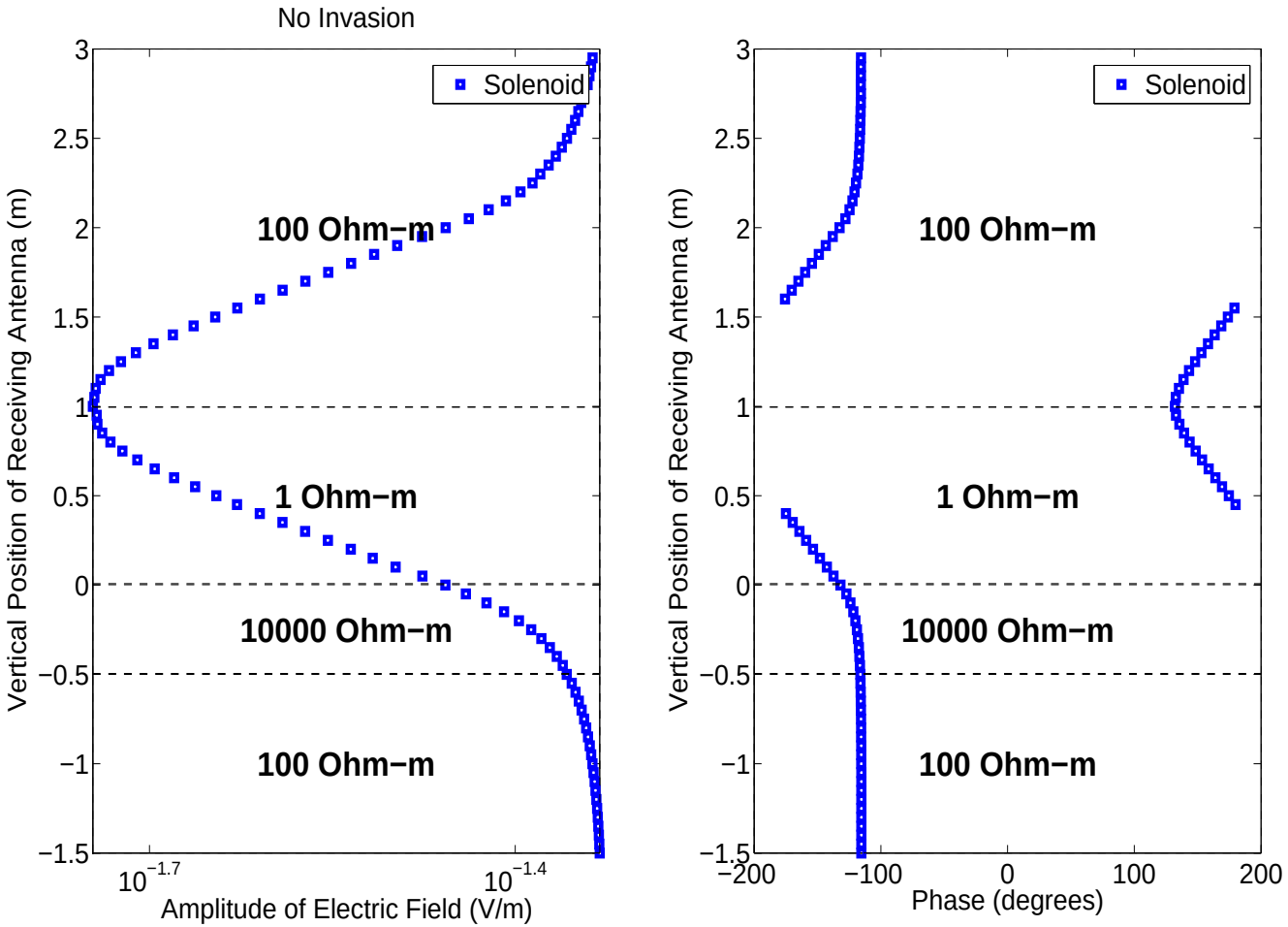

NUMERICAL RESULTS

H_ϕ for different antennas

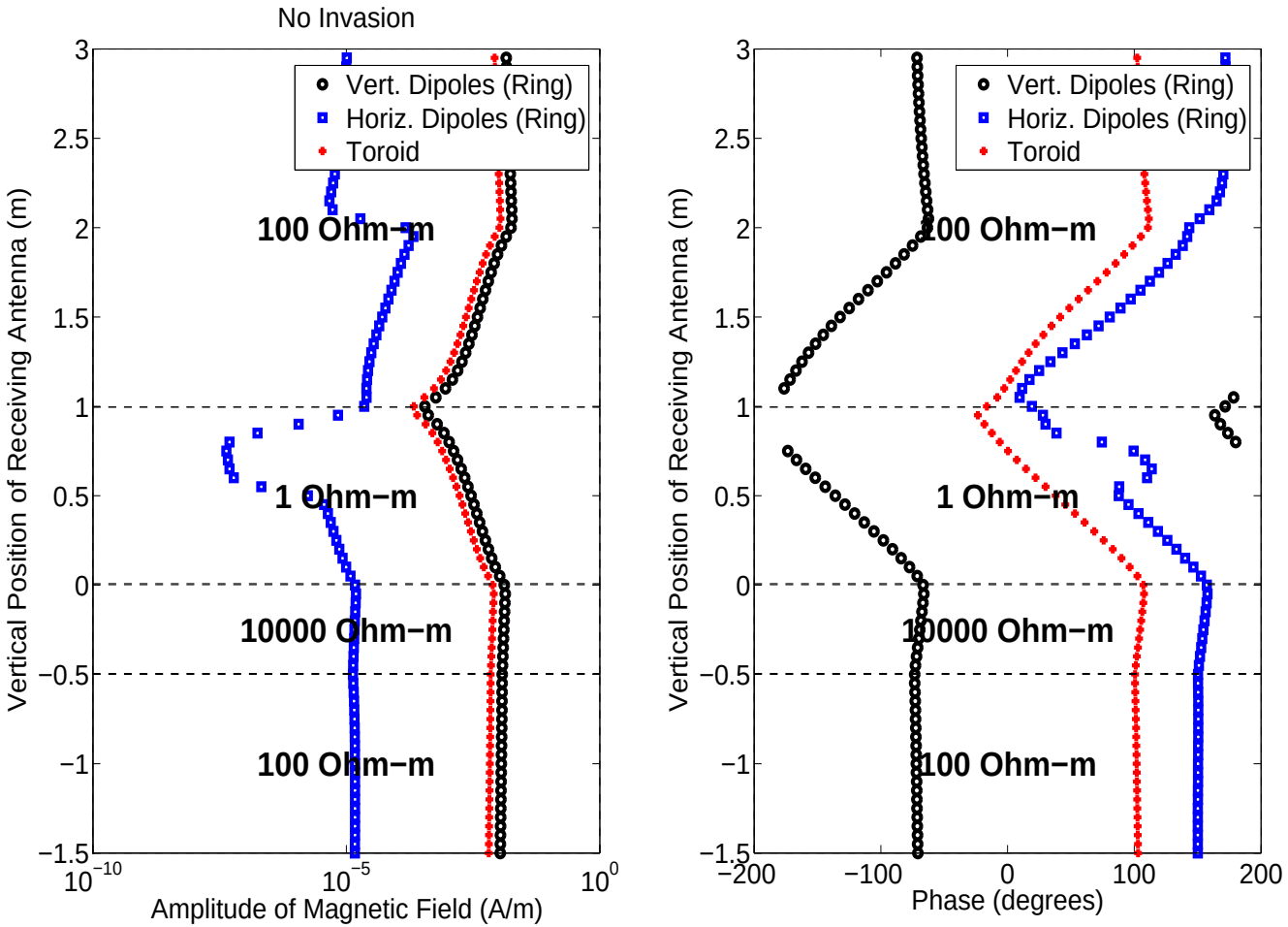

NUMERICAL RESULTS

First Vert. Diff. H_ϕ for different antennas

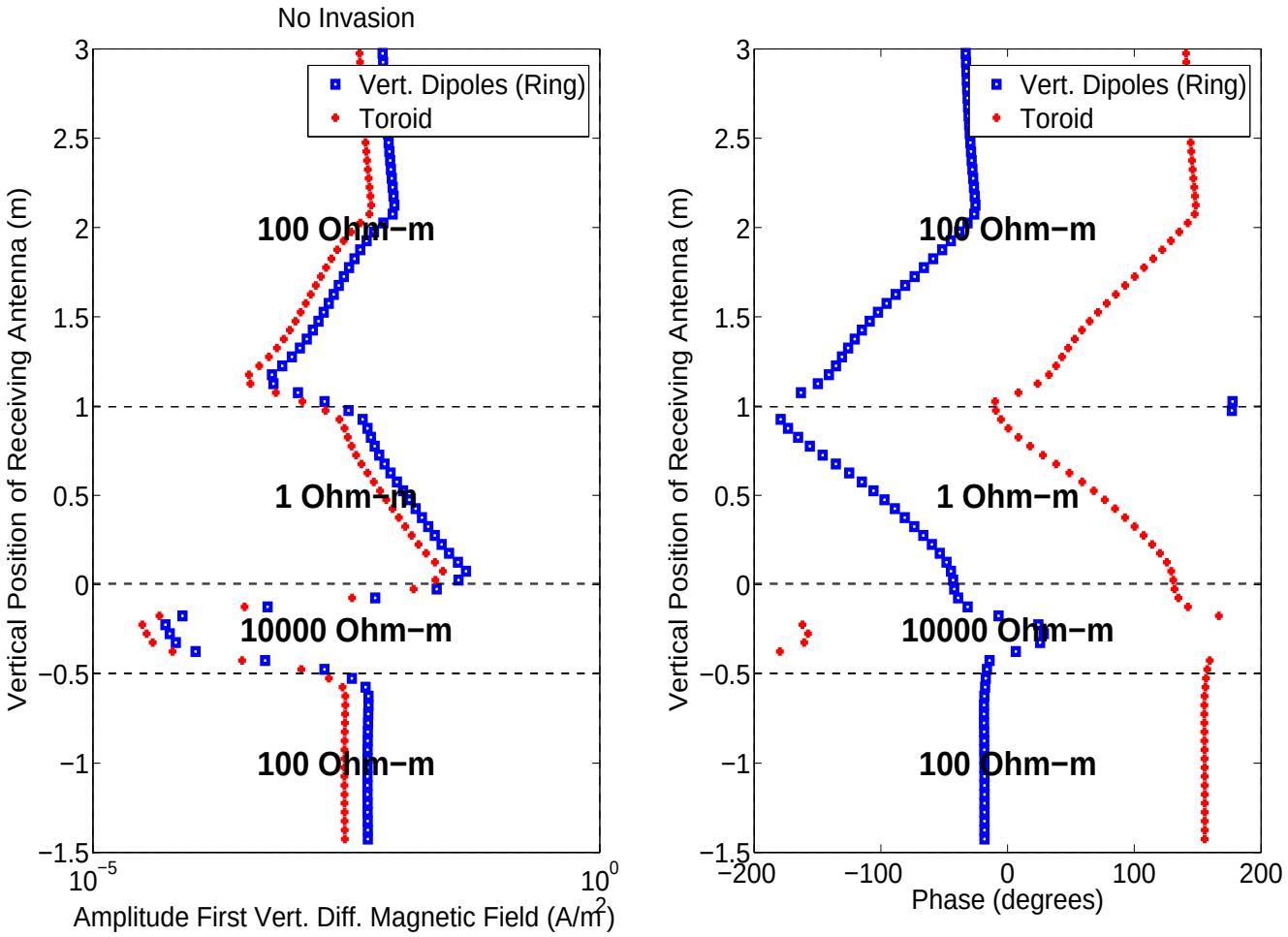

NUMERICAL RESULTS

First Vert. Diff. E_z for a toroid antenna

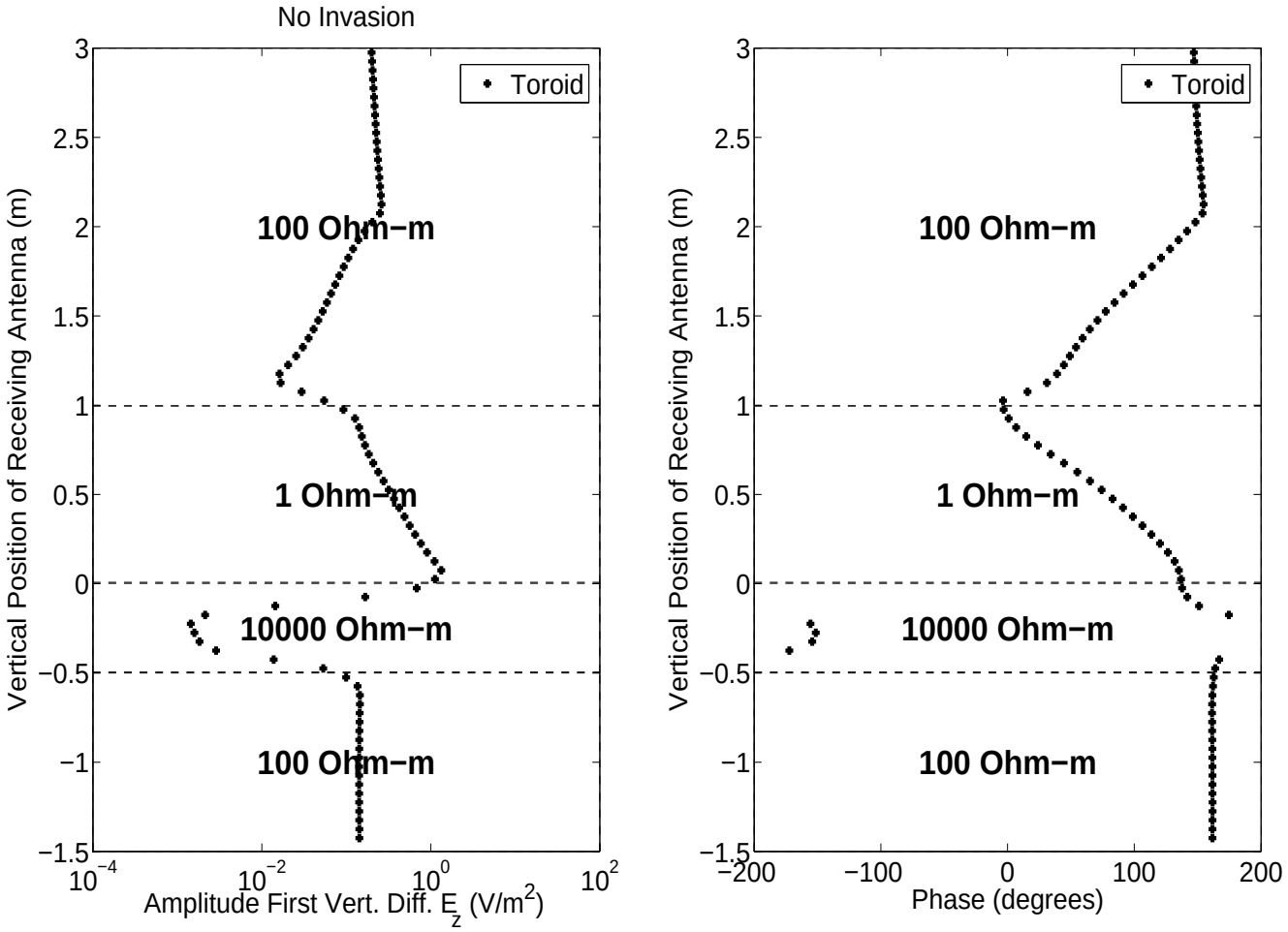

NUMERICAL RESULTS

First Vert. Diff. H_z for a solenoid antenna

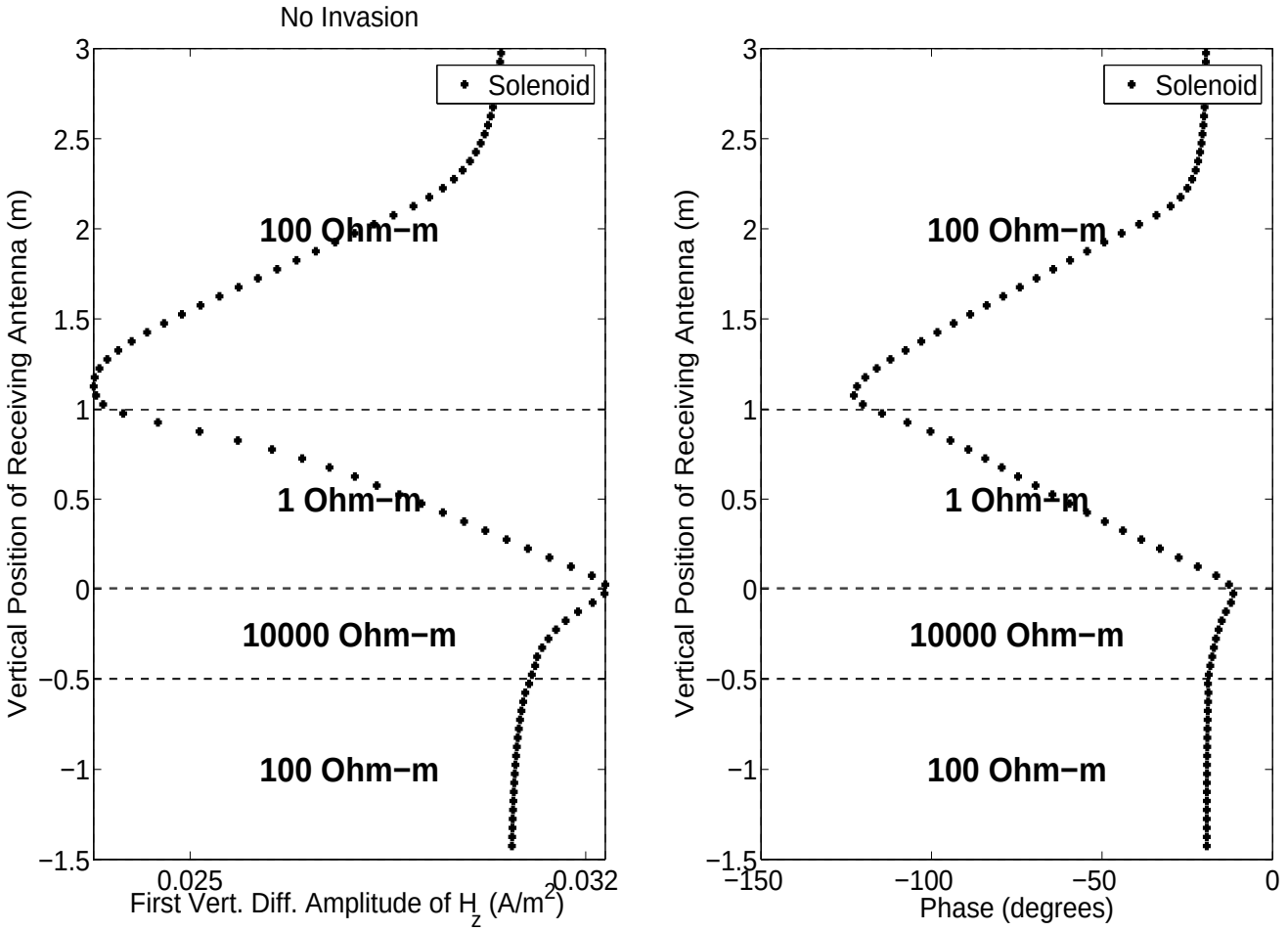

NUMERICAL RESULTS

First Vert. Diff. E_ϕ for a solenoid antenna

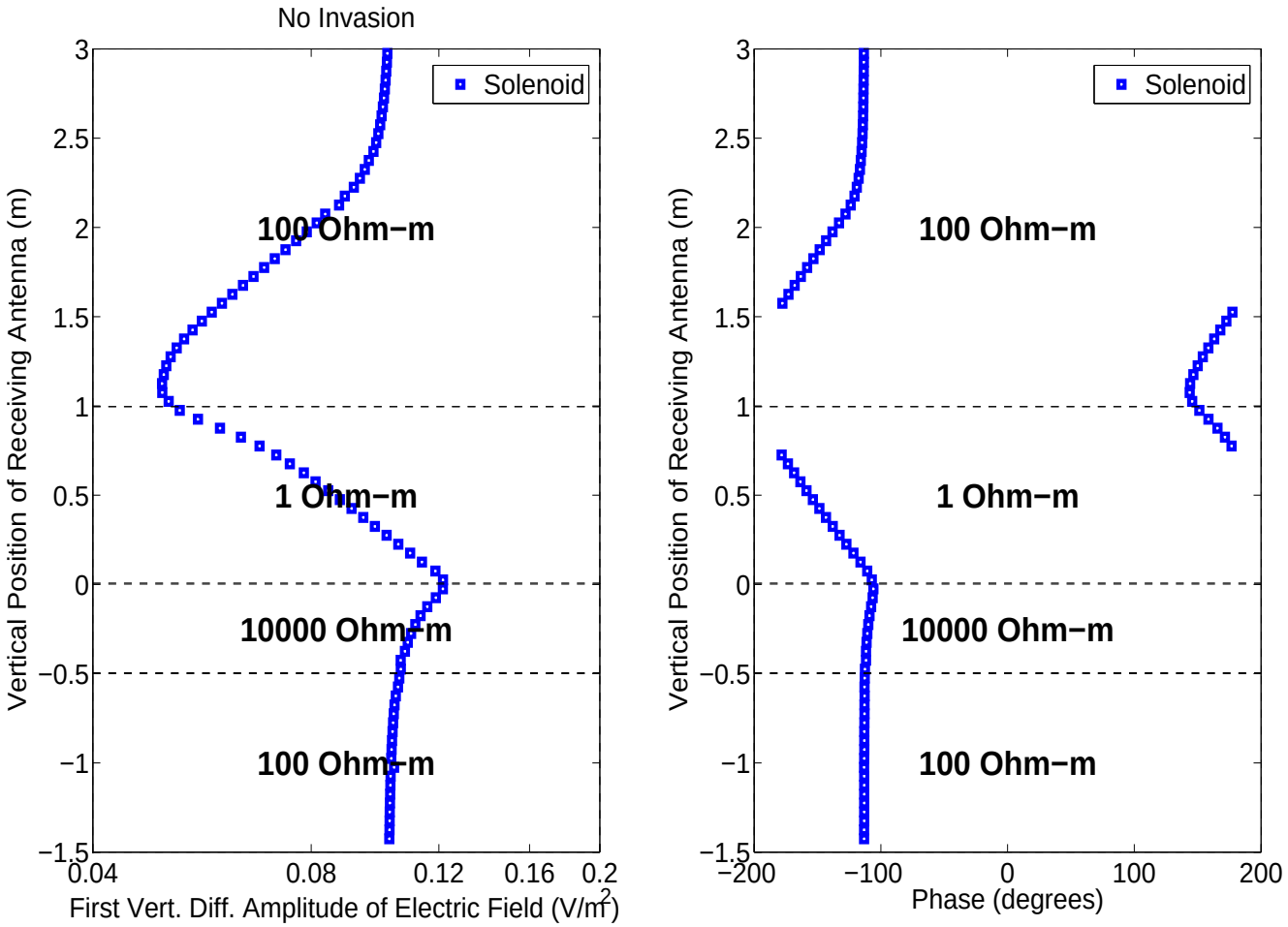

NUMERICAL RESULTS

Use of Magnetic Buffers (E_ϕ for a solenoid)

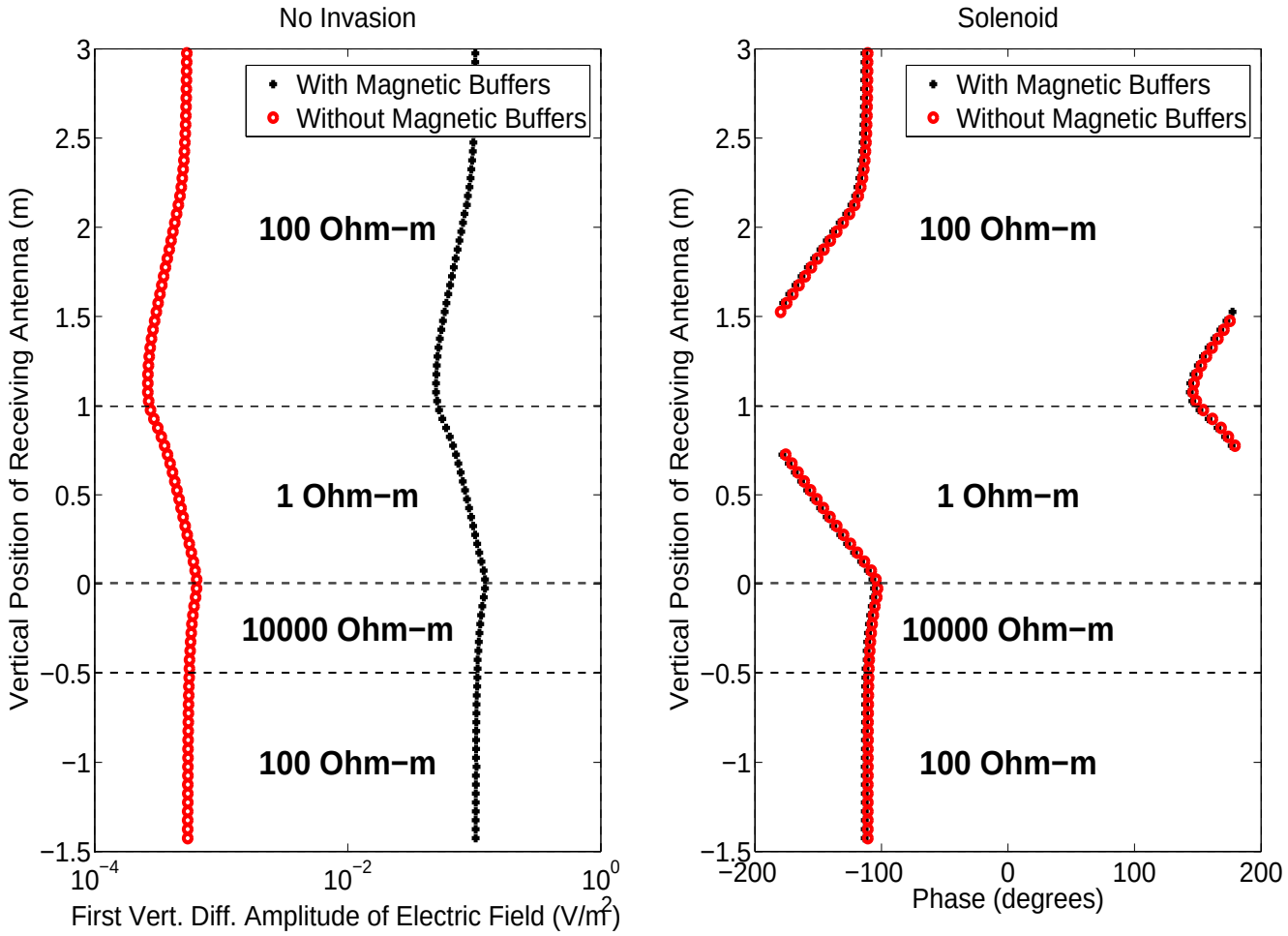

NUMERICAL RESULTS

Use of Magnetic Buffers (H_ϕ for a toroid)

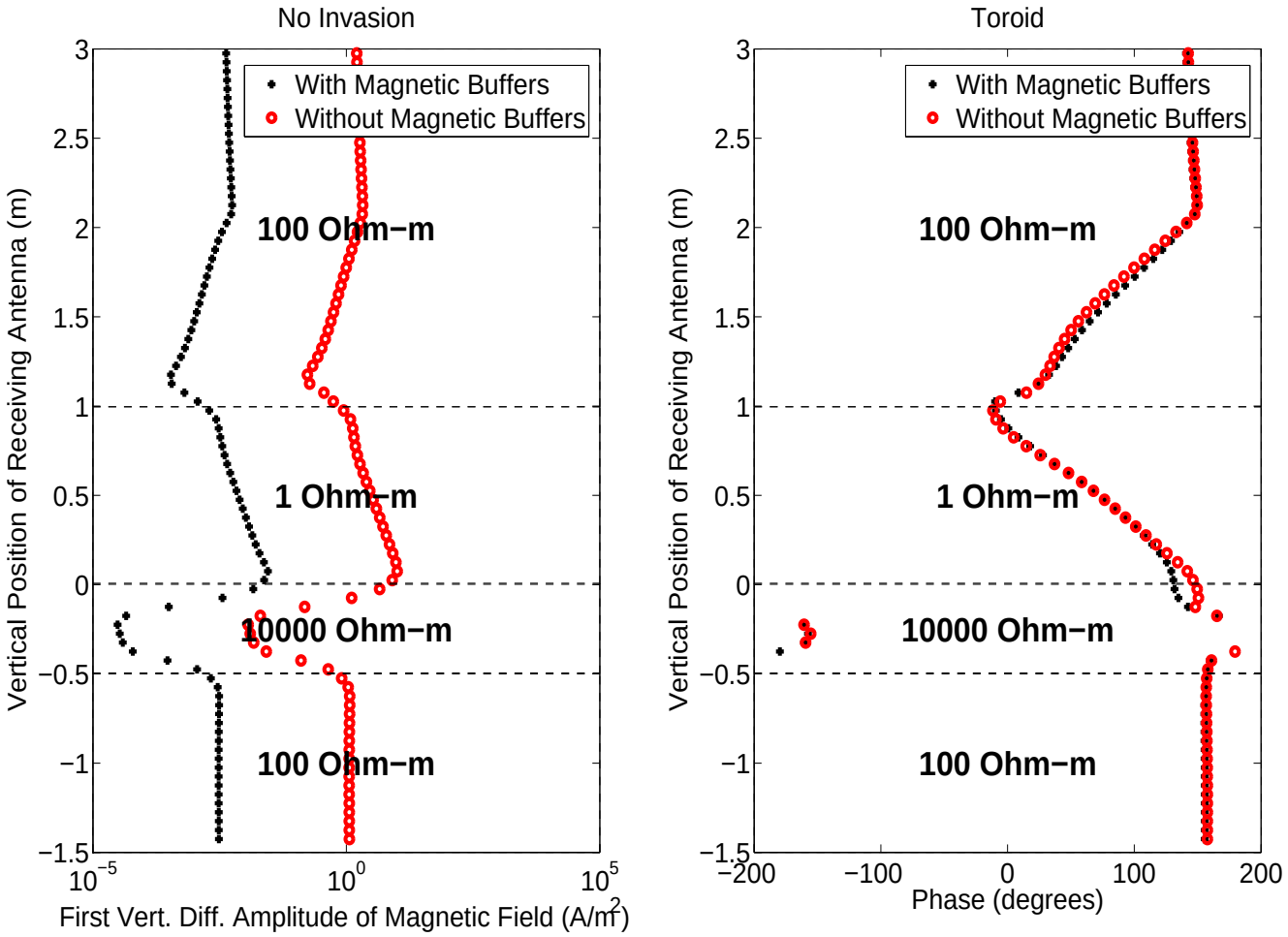

NUMERICAL RESULTS

Invasion study (E_ϕ for a solenoid)

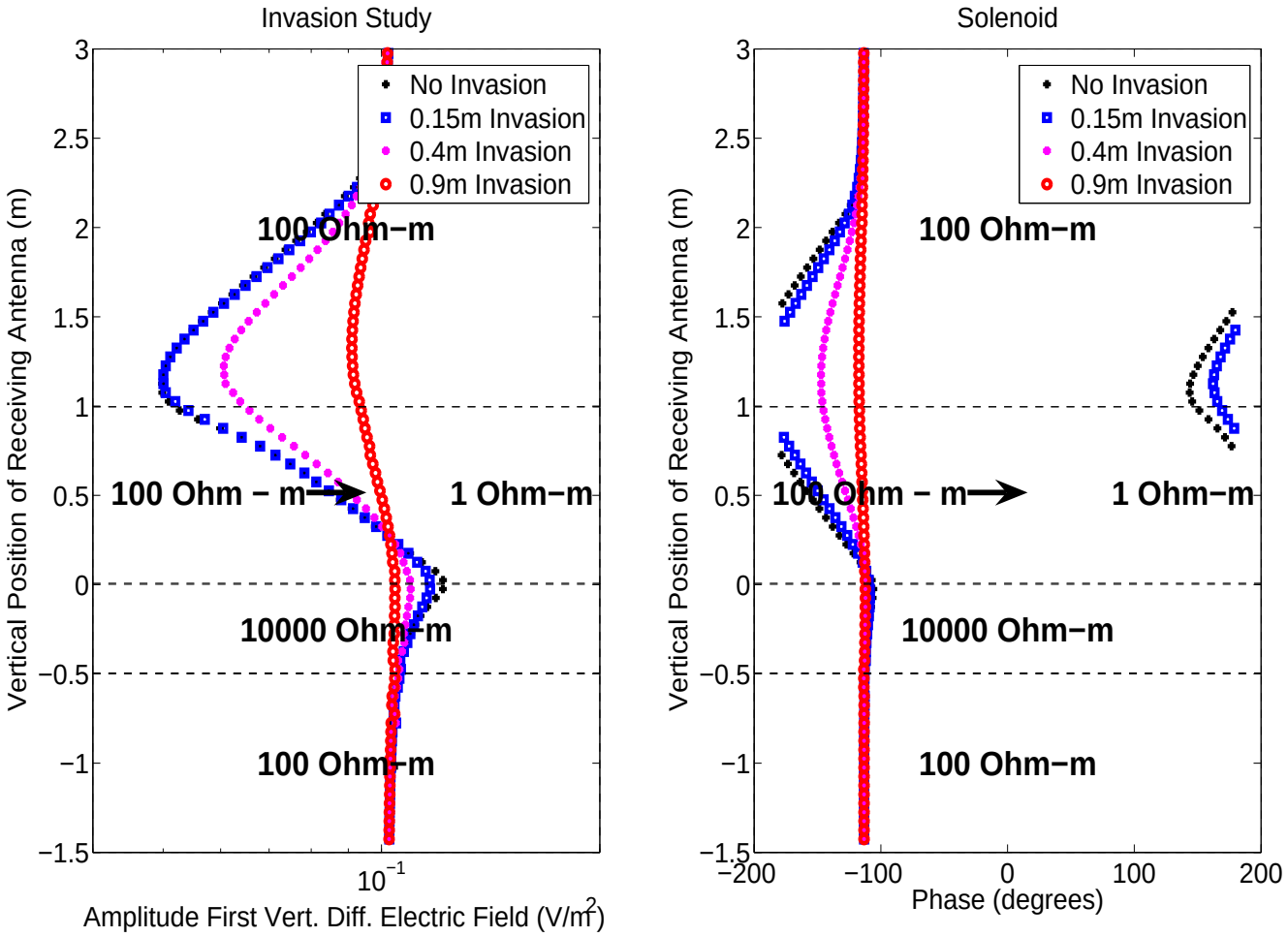

NUMERICAL RESULTS

Invasion study (H_ϕ for a toroid)

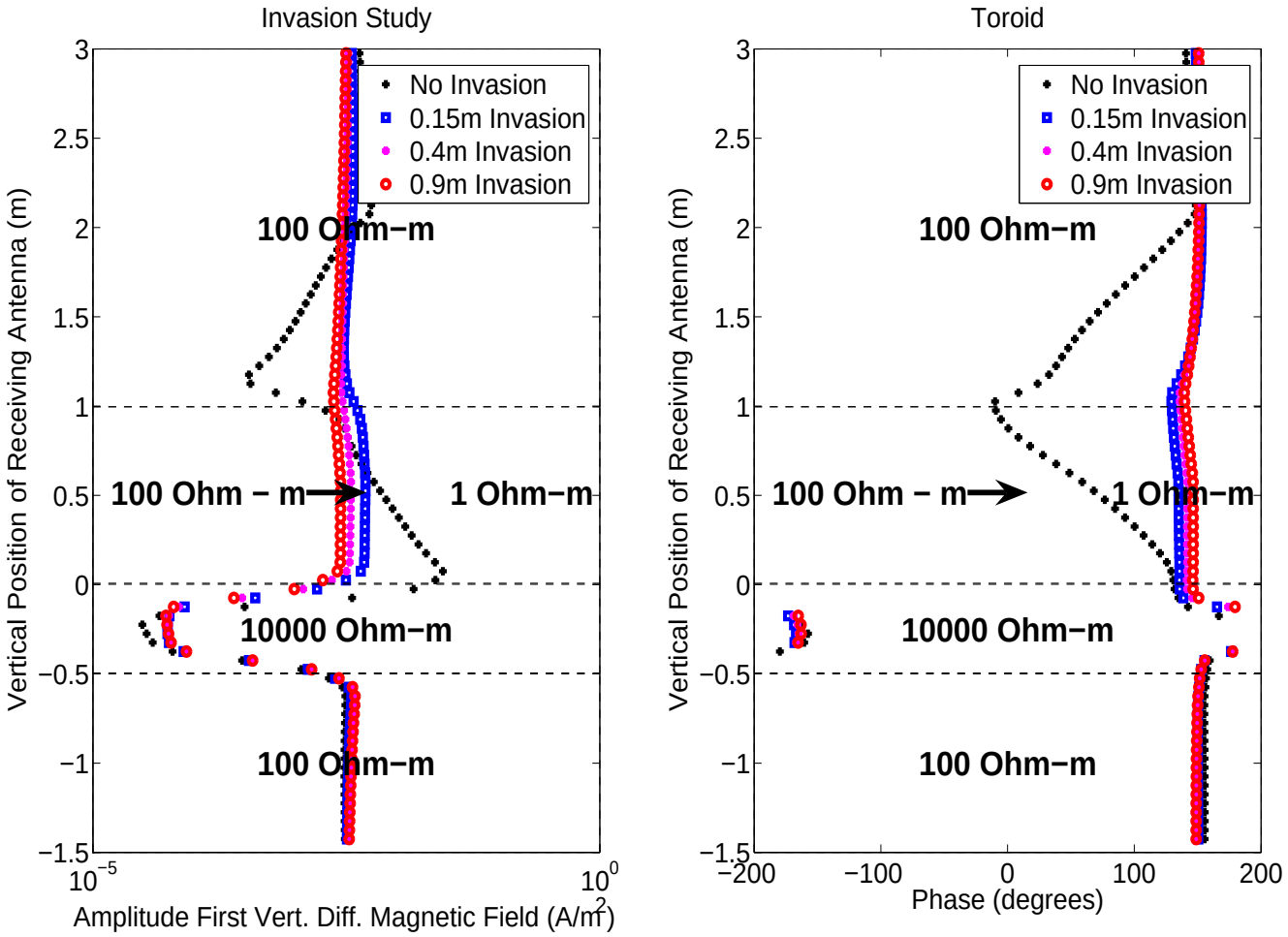

NUMERICAL RESULTS

Invasion study (E_ϕ for a solenoid)

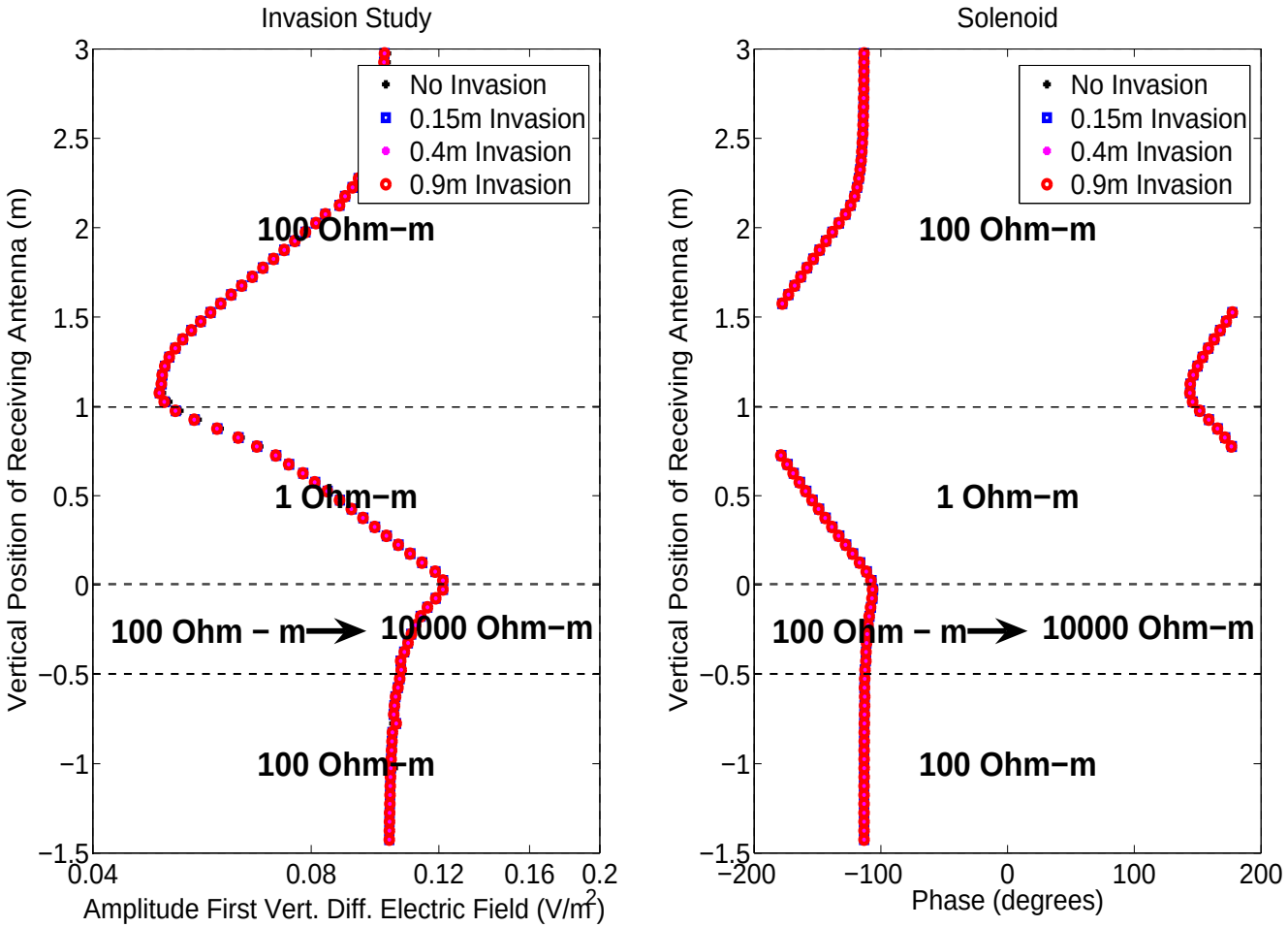

NUMERICAL RESULTS

Invasion study (H_ϕ for a toroid)

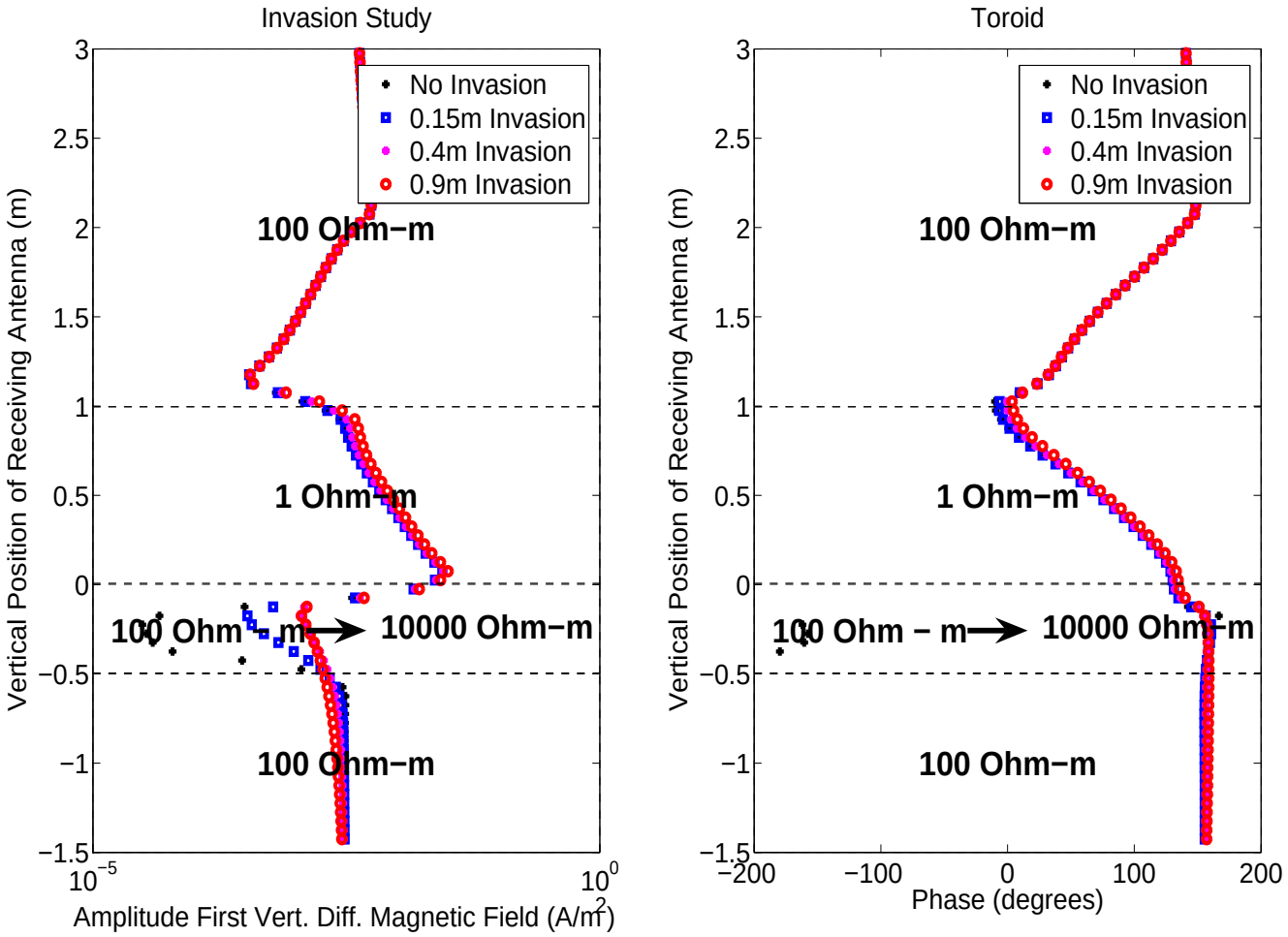

NUMERICAL RESULTS

Invasion and mandrel magnetic permeab. (E_ϕ)

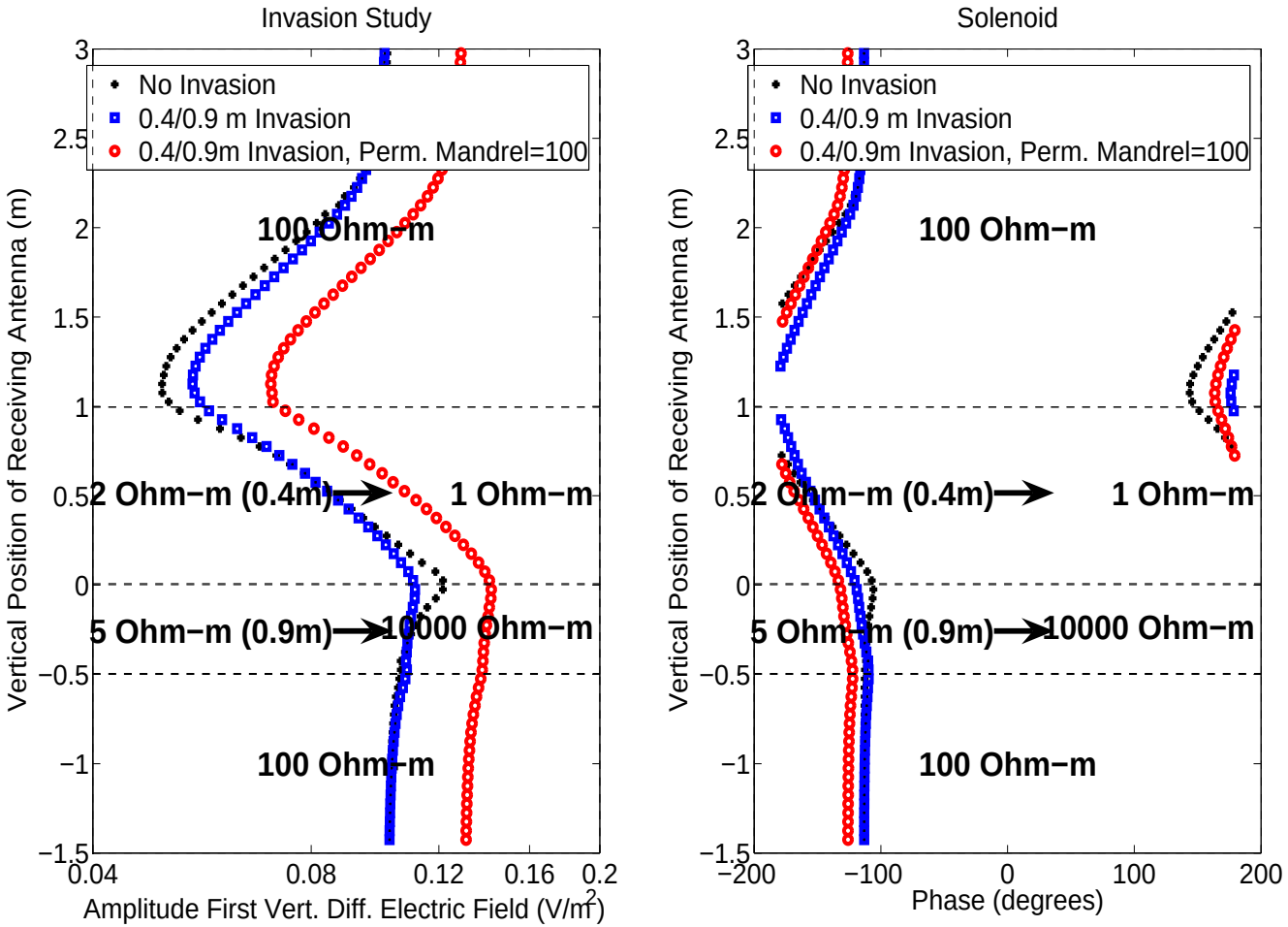

NUMERICAL RESULTS

Invasion and mandrel magnetic permeab. (H_ϕ)

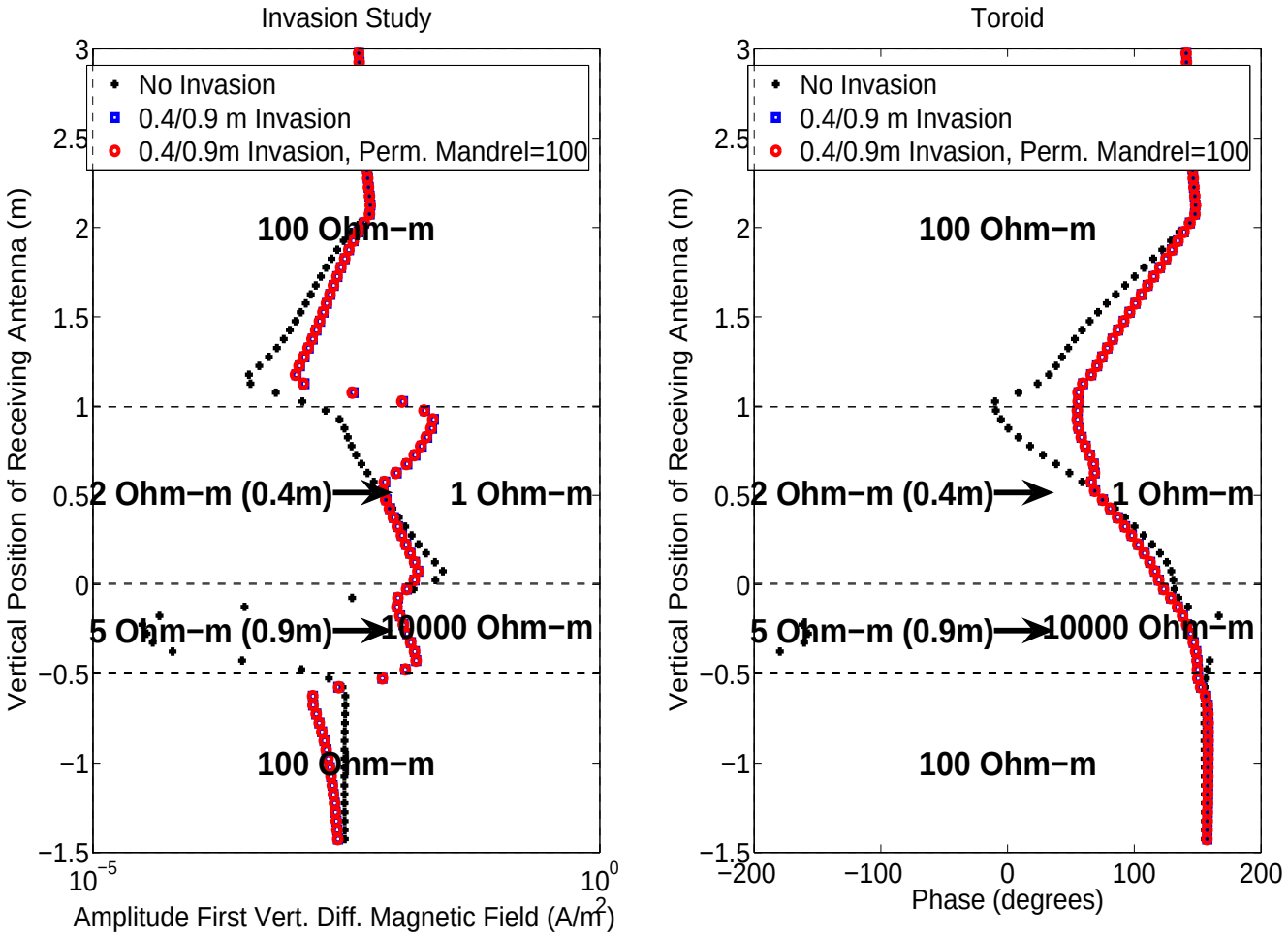

NUMERICAL RESULTS

Anisotropy (H_ϕ)

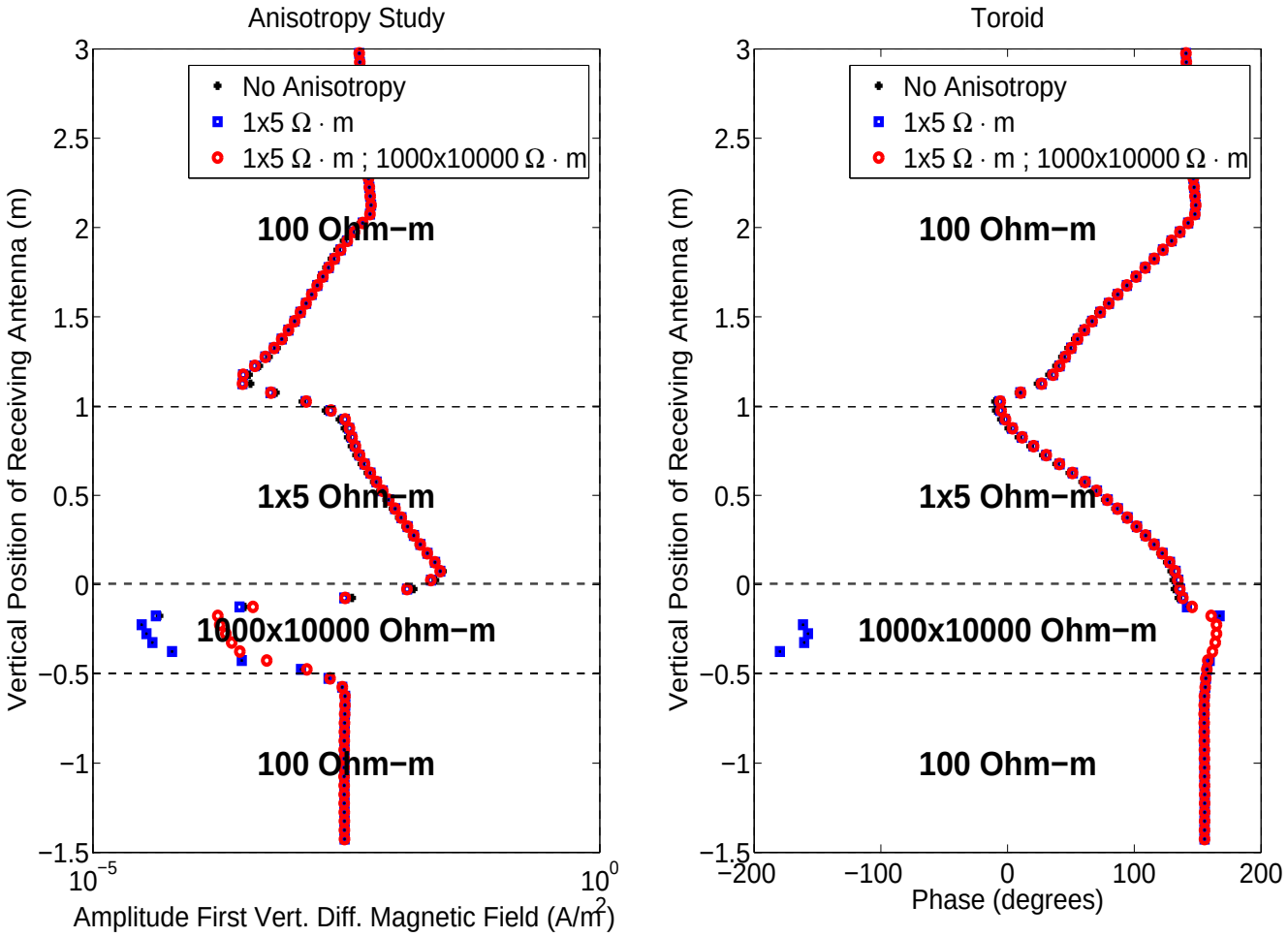

NUMERICAL RESULTS

Model Problem with Steel Casing

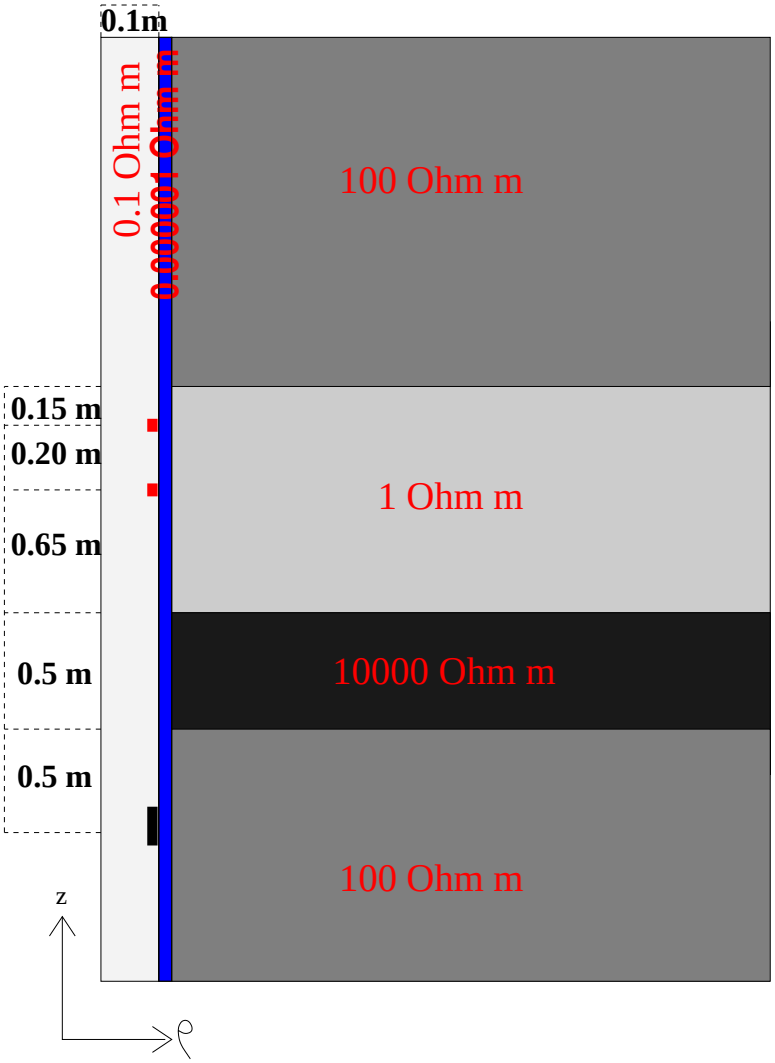

Frequency: 10 Hz - 10 kHz.

Casing resistivity: 10^{-6} Ohm · m.

Casing width: 0.01127 m

Discretization error $<$ 0.1 %

Toroidal antennas

Size (domain): 500m x 4000m

NUMERICAL RESULTS

Reliability (Can We Trust the Solutions?)

Problem with casing at 10 kHz.

Continuous Elements

Quantity of Interest	Real Part	Imag Part
COARSE GRID	0.1516098429E-08	-0.1456374493E-08
FINE GRID	0.1516094029E-08	-0.1456390824E-08

Edge Elements

Quantity of Interest	Real Part	Imag Part
COARSE GRID	0.1516060872E-08	-0.1456337248E-08
FINE GRID	0.1516093804E-08	-0.1456390864E-08

Error control provided by the fine grid solution.

NUMERICAL RESULTS

Reliability (Can We Trust the Solutions?)

Problem with casing at 10 kHz.

Continuous Elements

Quantity of Interest	Real Part	Imag Part
COARSE GRID	0.151609 8429E-08	-0.145637 4493E-08
FINE GRID	0.151609 4029E-08	-0.145639 0824E-08

Edge Elements

Quantity of Interest	Real Part	Imag Part
COARSE GRID	0.151606 0872E-08	-0.145633 7248E-08
FINE GRID	0.151609 3804E-08	-0.145639 0864E-08

Comparison between continuous elements vs. edge elements.

NUMERICAL RESULTS

Accuracy (Are the Solutions Accurate?)

Problem with Casing (Convergence Curve)

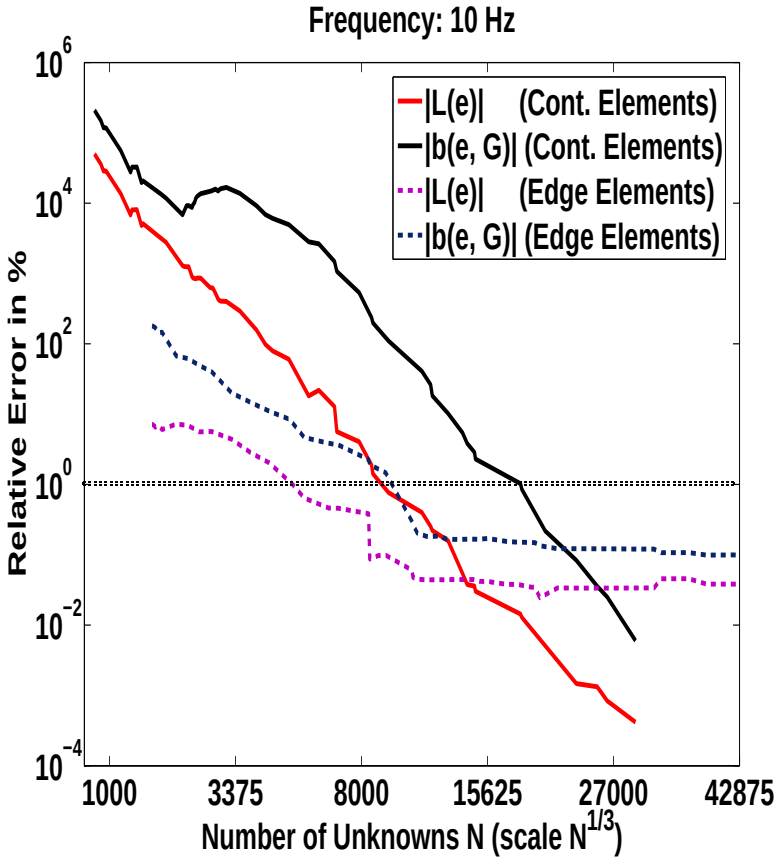

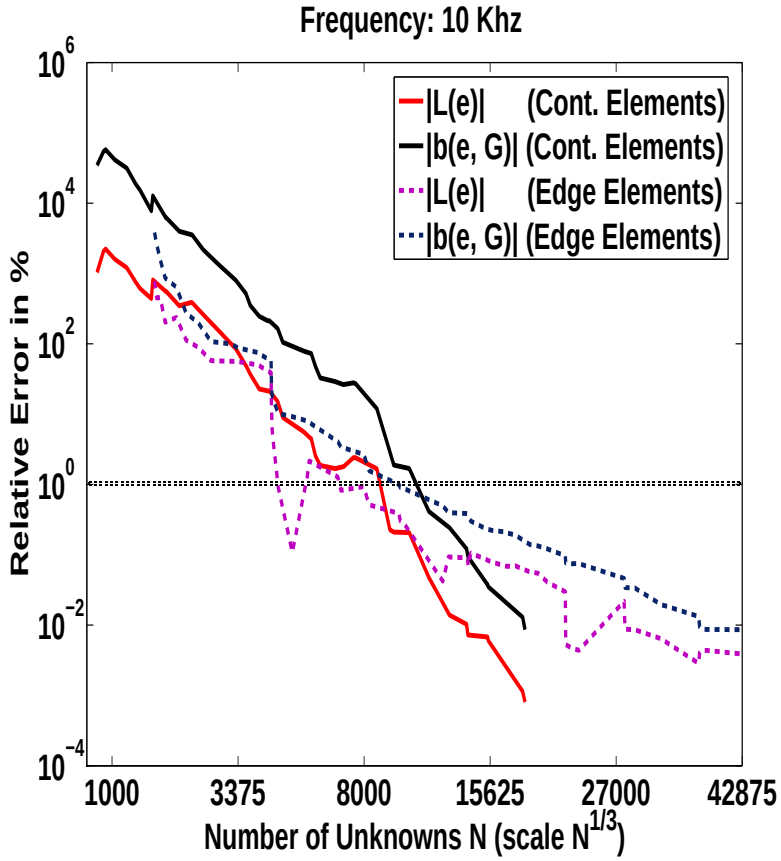

EXTREMELY ACCURATE SOFTWARE

NUMERICAL RESULTS

Performance (How Fast Can We Solve the Problems?)

80 Vert. Pos.	$10^{-6}\Omega \cdot m$	$10^{-5}\Omega \cdot m$
Toroid (10 Khz)	19' 46"	16' 28"
Ring of Vert. Dipoles (10 Khz)	22' 47"	17' 02"
Ring of Horiz. Dipoles (10 Khz)	19' 25"	13' 25"
Electrodes (0 Hz)	10' 10"	8' 35"

IBM Power 4 compiler 1.3 Ghz (4 years old)

Possible improvements in performance:

- To use a 3.4 Ghz processor.
- To execute the code in 8 processors (10 positions per processor).
- To improve implementation.

HIGH PERFORMANCE SOFTWARE

NUMERICAL RESULTS

First Difference of Electric Field at Different Frequencies

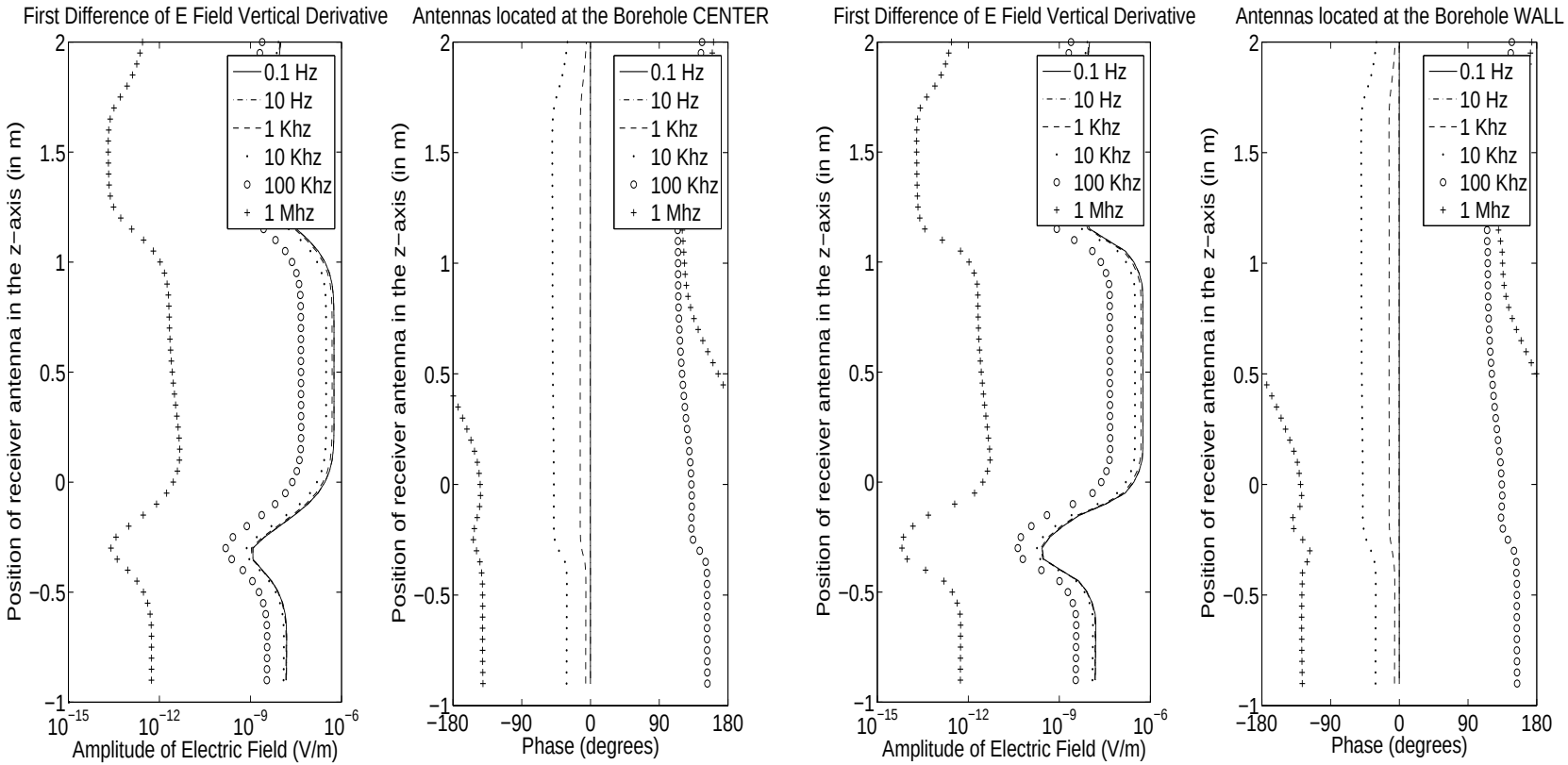

Toroid antennas are more sensitive to the rock formation resistivity when located on the borehole's wall

NUMERICAL RESULTS

First Difference of Magnetic Field at Different Frequencies

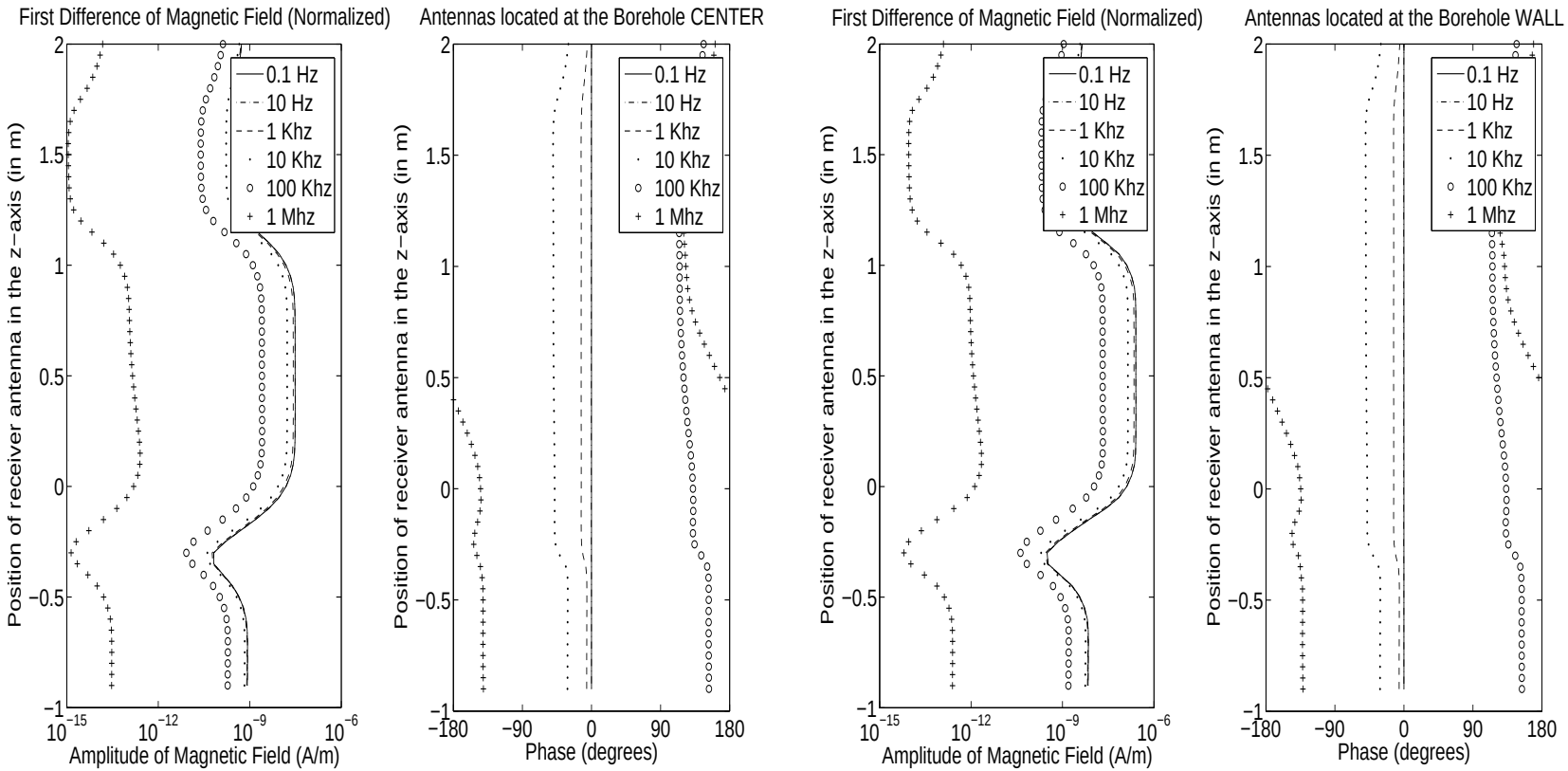

NUMERICAL RESULTS

Electromagnetic Fields at Different Frequencies

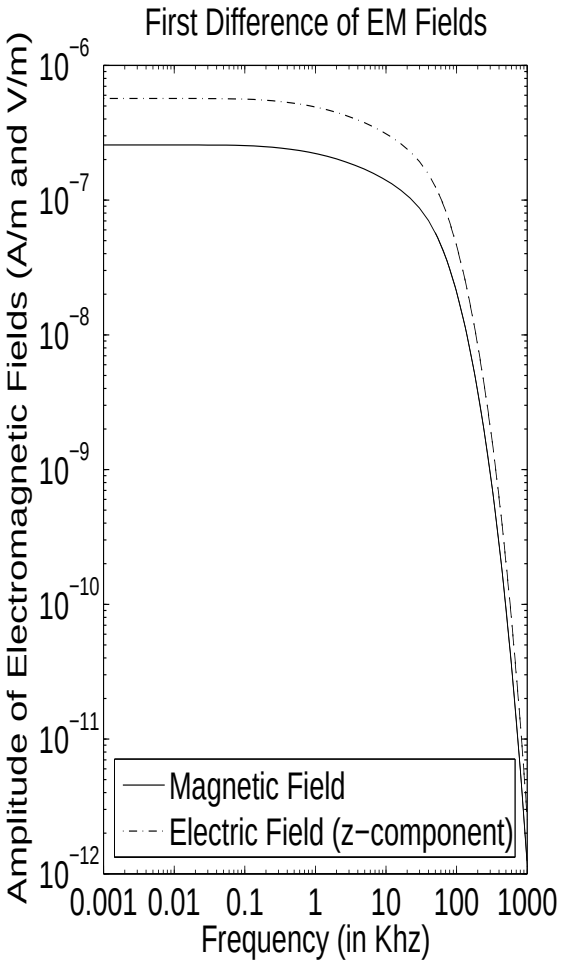

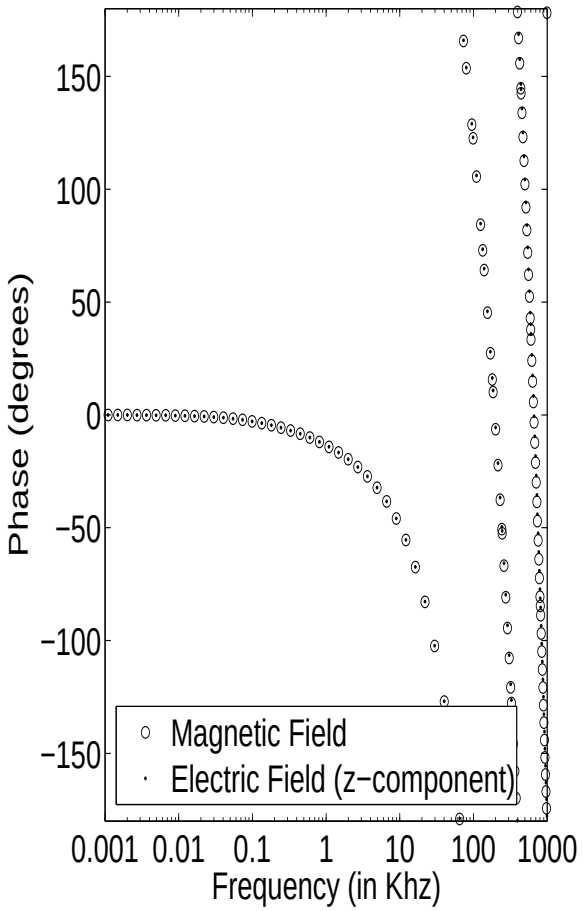

Electromagnetic Fields are almost constant for frequencies below 1 kHz. A sudden drop in the amplitude occurs at frequencies above 20 kHz.

CONCLUSIONS AND FUTURE WORK

- The self-adaptive goal-oriented hp-adaptive strategy converges exponentially in terms of a user-prescribed quantity of interest vs. the CPU time.
- We obtain fast, reliable and accurate solutions for problems with a large dynamic range and high material constrasts.

Future Work

- To apply the self-adaptive goal-oriented hp-FEM to 3D problems for simulation of deviated wells.
- To apply the self-adaptive goal-oriented hp-FEM for inversion of 2D multi-physic problems.

Department of Petroleum and Geosystems Engineering, and
Institute for Computational Engineering and Sciences (ICES)